H. H. Gorris and O. S. Wolfbeis

DOI: 10.1002/anie.201208196

Photon Upconversion

Photon-Upconverting Nanoparticles for Optical Encoding and Multiplexing of Cells, Biomolecules, and Microspheres

Hans H. Gorris and Otto S. Wolfbeis*

Keywords:
anti-Stokes emission · lanthanides · nanoparticles · optical encoding · photon upconversion

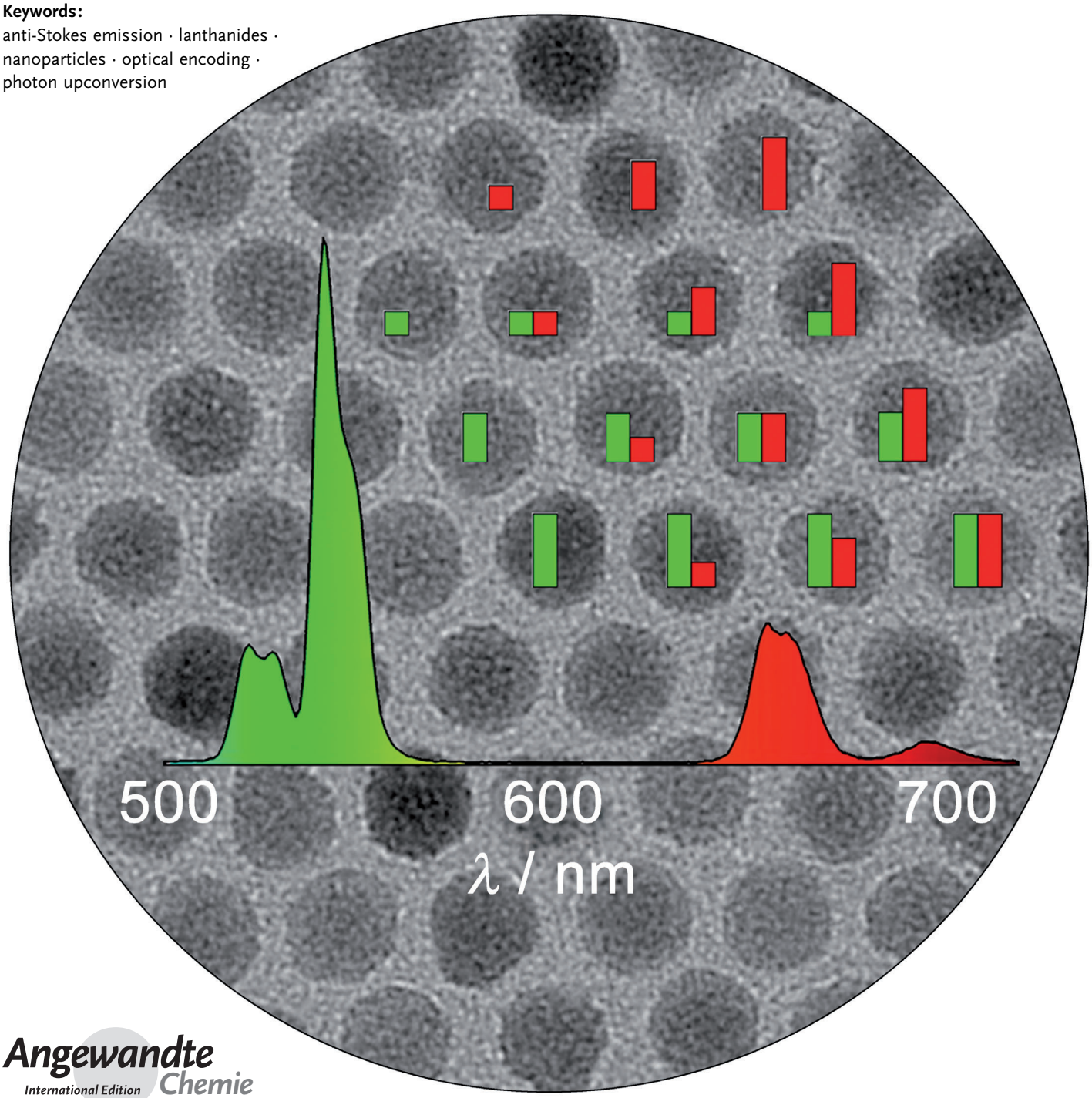

Photon-upconverting nanoparticles (UCNPs) are lanthanide-doped nanocrystals that emit visible light under near-infrared excitation (anti-Stokes emission). This unique optical property precludes background fluorescence and light scattering from biological materials. The emission of multiple and narrow emission lines is an additional hallmark of UCNPs that opens up new avenues for optical encoding. Distinct emission signatures can be obtained if the multiple emission of UCNPs is tuned by their dopant composition or by surface modification with dyes. Tuning the intensity of only one of the multiple emission lines and using another one as a constant reference signal enables the design of ratiometric codes that are resistant to fluctuations in absolute signal intensities. Combining several UCNPs each displaying a distinct set of emission lines expands the coding capacity exponentially and lays the foundation for highly multiplexed analyte detection. This Review highlights the potential of UCNPs for labeling and encoding biomolecules, microspheres, and even whole cells.

From the Contents

1. Introduction 3585
2. Features of Photon-Upconverting Nanoparticles for Multiplexed Encoding 3586
3. Multicolor Tuning of UCNPs by the Material Composition 3588
4. Multicolor Tuning of UCNPs by an Optical Surface Layer 3590
5. Multiparameter Encoding 3591
6. Synthesis and Surface Modification of Biocompatible UCNPs 3592
7. Multicolor-Labeling of Cells with UCNPs for Bioimaging 3593
8. Spatially Encoded Heterogeneous Bioassays 3594
9. Microsphere-Encoded Heterogeneous Bioassays 3595
10. Multiplexed Homogeneous Assays 3595
11. Multiple Chemical Sensing 3596
12. Summary and Outlook 3596

1. Introduction

The development of new encoding strategies is a driving force for multiplexed analyte detection in complex mixtures with minimized sample volume, assay time, and cost. Multiplexed analyte detection enables genotyping,[1] medical diagnosis,[2] screening of combinatorial libraries,[3] and environmental monitoring.[4] Two multiplexed assay formats can be broadly distinguished: In the first, a multitude of probe elements is identified by the spatial position on planar arrays.[5] In the second, the probes are attached to suspended microspheres that are labeled with an identifier code or "barcode".[6] Microspheres in suspension have a large surface area and enable fast binding kinetics. Whereas planar arrays have to be spotted individually, encoded microspheres can be generated faster and more homogeneously in large batch syntheses.[7] Thus, encoded microspheres have the potential to greatly reduce the costs per array, provided they can be detected using simple and inexpensive instrumentation. Encoded microspheres[8,9]—and even cells[10]—benefit from higher flexibility because they can be sorted in suspension using flow cytometry or assembled into arrays of femtoliter wells.[11,12] Both modes of detection allow for screening a large number of different probe elements in parallel. In addition, each type of encoded microsphere is present in multiple copies, which allows the observation of a statistically relevant number of probe elements in a single experiment.

The maximal degree of multiplexing based on the use of (suspended) microspheres depends on the number of identifier codes that can be detected separately. Various optical encoding strategies have been described to obtain as many codes as possible. Graphical encoding, for example, uses two-dimensional patterns on microparticles as barcodes.[13–18] Defining and resolving optical patterns on a micrometer scale, however, relies on sophisticated instrumentation. In contrast, spectral encoding, exploits either characteristic IR or Raman spectra fingerprints as encoding elements[19–24] or the emission spectra and intensities of luminescent materials, such as fluorescent dyes, quantum dots, or photon-upconverting nanoparticles. The labeling of microparticles with fluorophores is probably the most established method for spectral encoding.[8,25] Microspheres, usually made from polystyrene, can be swollen in an organic solvent containing defined concentrations of fluorophores. Following the transfer of the microparticles to an aqueous solution, they shrink and permanently enclose the fluorophores.

Spectral encoding is compatible with standard optical detection schemes, such as flow cytometry and is thus widely applicable. Equation (1) gives the maximal number of spectral codes (C)

$$C = i^w - 1 \quad (1)$$

[*] Dr. H. H. Gorris, Prof. O. S. Wolfbeis
Institute of Analytical Chemistry, Chemo- and Biosensors
University of Regensburg
93040 Regensburg (Germany)
E-mail: hans-heiner.gorris@ur.de

where i is the number of intensity levels that can be differentiated and w is the number of wavelengths.[26] One intensity level always has to be subtracted as it is indistinguishable from the background. C can be increased exponentially by using multiple intensity levels and multiple wavelengths at the same time. For example, four intensity levels and two wavelengths result in a coding capacity of 15 ($=4^2-1$; Figure 1), while ten intensity levels and four wavelengths in principle yield 9999 codes. The actual coding capacity, however, is limited because of a) the width and overlap of emission spectra, b) variations in intensity levels, and c) interfering background signals.

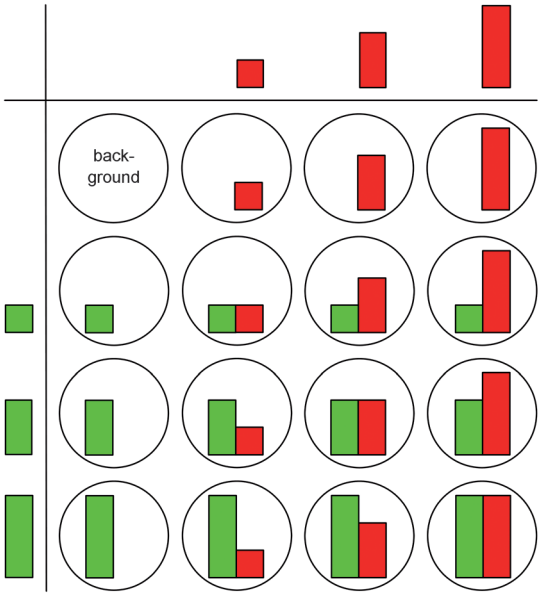

Figure 1. Schematic representation of an encoding scheme. Microspheres are labeled with combinations of two fluorescent dyes that emit either green or red light. The emission intensity of each dye can be modulated individually by adjusting their concentrations. Microspheres that contain no fluorophore cannot be distinguished from the background. Thus, a combination of two colors and four intensity levels yields 15 ($=4^2-1$) codes.

Several approaches have been investigated to extend the limited number of codes that can be generated from conventional fluorophores. For example, the emission of fluorophore-doped silica nanoparticles can be modulated by tuning the efficiency of fluorescence resonance energy transfer to various acceptors.[27] Additional information is provided by fluorescence lifetime data.[28] Finally, a combinatorial code can be generated by using a biomolecule, such as DNA as the encoding element. In this case, a specific DNA barcode is attached to each microsphere. The DNA barcode can then be decoded through sequential hybridization and dehybridization steps using complementary oligonucleotides that carry different fluorophores.[29,30]

Nanoparticle-based codes have distinct advantages over conventional organic fluorophores because they are widely resistant to photobleaching and their emission spectra can be fine-tuned by the design of the nanoparticle. For example, the surface structure of gold nanoparticles can be modulated to obtain characteristic resonance wavelengths for multiplexed encoding on surface plasmon resonance platforms.[31–36] Luminescent nanoparticles, on the other hand, can be used for spectral encoding in the same way as organic fluorophores. Quantum dots of the type (Cd/Zn)Se display size-dependent emission colors[26,37,38] which allows a series of coding elements to be generated. Excitation light of a single wavelength—typically in the UV—can be employed to read out all the codes simultaneously.[39,40] Biological applications of quantum dots, however, are hampered by the toxicity of cadmium(II) and because short-wavelength excitation leads to fairly strong background fluorescence of biomaterials.

These shortcomings can be elegantly avoided by using a relatively new class of nanoparticles, the so-called photon-upconverting nanoparticles (UCNPs). While the properties and potential of UCNPs have been reviewed recently,[41–43] our Review focuses on how their unique luminescent features can be exploited for designing new encoding strategies.

2. Features of Photon-Upconverting Nanoparticles for Multiplexed Encoding

Efficient spectral encoding strategies for multiplexed analysis of biological samples depend on both low background signals from biomolecules and good separation of emission signals to distinguish as many codes as possible. Background interference is particularly a concern when using short-wavelength light. Rayleigh scattering is strongest in the UV range and decreases with the fourth power of the

Hans-Heiner Gorris studied biology at the University of Münster, Germany, and the University of York, UK. He received his PhD with Dr. Andreas Frey from the University of Lübeck in 2005. After working on single-enzyme molecule kinetics in optical-fiber bundle arrays with Prof. David Walt at Tufts University, USA he joined the Faculty of Chemistry and Pharmacy at the University of Regensburg (2009) and established his research group "Bioanalysis on the Micro- and Nanometer scale". His research is focused on ultrasensitive detection methods for bioanalysis.

Otto S. Wolfbeis is a Professor of Analytical and Interface Chemistry at the University of Regensburg. His research focuses on optical (fiber) chemical sensors, fluorescence spectroscopy and imaging, on fluorescent probes and labels, and on luminescent nanomaterials. He has published over 500 scientific articles and Reviews. He was the Founding Editor of the Springer Series on Fluorescence, is the Editor-in-Chief of Microchimica Acta, and one of the ten curators of Angewandte Chemie.

wavelength. Many biomolecules show strong autofluorescence under short-wavelength illumination.[44] At the other end of the spectrum, there is little interaction between near-infrared (NIR) light and biomaterials. Consequently, NIR light hardly induces any background luminescence or photodamage. NIR light also penetrates deeply into biological materials, which allows multilayered biological samples to be interrogated. Several strategies have been developed to exploit the advantages of long-wavelength excitation. The simplest option is the use of long-wavelength absorbing organic fluorophores.[45] The quantum yields of organic dyes, however, typically decrease at longer-wavelength absorption maxima. Non-linear optics, in contrast, allows organic fluorophores[46] or quantum dots[47] to be excited with two or more long-wavelength photons and detecting the emissions that occur at shorter wavelengths (so-called anti-Stokes emission). The most common types of anti-Stokes processes, two-photon excitation[48,49] and second harmonic generation,[50] rely on high photon flux intensities because of the need for simultaneous absorption of two photons or the combination of two photons, respectively, which are extremely rare events. Therefore, expensive and powerful pulsed lasers are required that may exert adverse effects on biomaterials.

Photon-upconverting nanoparticles (UCNPs) are inorganic nanocrystals that allow for the generation of anti-Stokes emission under more beneficial conditions. A continuous diode laser is adequate to cause the absorption of two or more photons of long-wavelength light. UCNPs then emit light of shorter wavelengths with large anti-Stokes shifts.[51] The most efficient UCNPs known to date consist of a hexagonal $NaYF_4$ host lattice (Figure 2) that is doped with low concentrations of trivalent ytterbium and erbium ions ($NaYF_4$: 20% Yb, 2% Er).[52–55] The hexagonal host lattice aligns the dopant ions to allow for an optimal energy transfer upconversion (ETU) mechanism between the f-orbitals of the Yb^{3+} and Er^{3+} ions, which have closely matching energy differences.[56] In addition, $NaYF_4$ is a host lattice of low phonon energy, which keeps multiphonon relaxation rates low and allows lifetimes of excited states up to the milliseconds range.[57] The long-lived metastable states of lanthanides explain why sensitization by ETU is about a factor of up to 10^6 more efficient than simultaneous two-photon excitation.

NIR light of 980 nm wavelength elevates the $^2F_{7/2}$ ground state of the sensitizer Yb^{3+} to the excited state $^2F_{5/2}$ (according to the Russel–Saunders spin-orbit coupling scheme)[58,59] with an energy difference of about $10^4\ cm^{-1}$ (Figure 3). The activator Er^{3+} is then sensitized in two sequential energy-transfer steps similar in size to those of Yb^{3+}. First, the ground state $^4I_{15/2}$ is elevated to the metastable state $^4I_{11/2}$. Owing to its long lifetime, the $^4I_{11/2}$ state can be strongly populated to allow for the second energy transfer step to form the $^4F_{7/2}$ multiplicity. Following multiphonon relaxation, the Er^{3+} ion emits green light from the states $^2H_{11/2}$ (521 nm) or $^4S_{3/2}$ (543 nm), respectively. Additional relaxation steps lead to the population of the $^4F_{9/2}$ state. The Er^{3+} ion then emits red light (657 nm). Consequently, the emission spectrum of UCNPs, type $NaYbF_4$:Er, displays mainly two (green and red) well-separated emission lines.

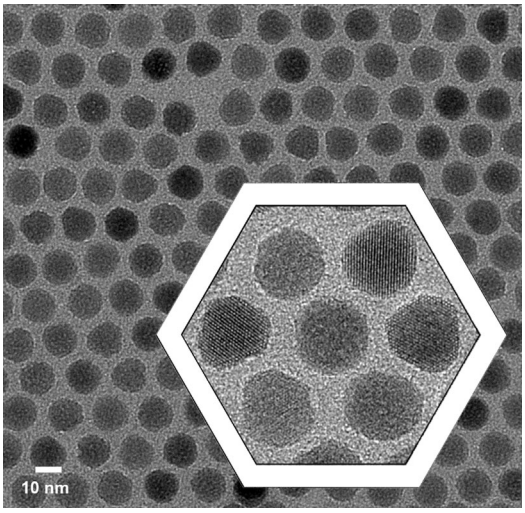

Figure 2. TEM image of UCNPs of type $NaYF_4$: 30% Gd, 18% Yb, 2% Er in 75000× magnification (160000× in the inset) revealing good monodispersity. The hexagonal crystal phase results in a hexagonal shape of the individual nanoparticles that assemble in a honeycomb pattern (highlighted in the inset).

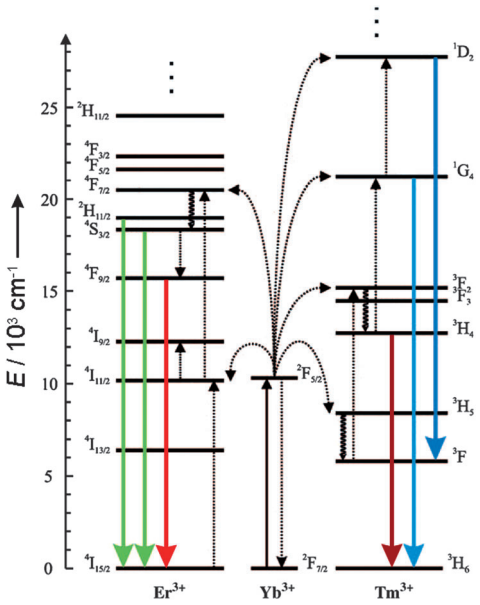

Figure 3. Schematic energy-level diagram of the anti-Stokes processes in UCNPs of type $NaYF_4$:Yb,Tm/Er. Embedded in a hexagonal $NaYF_4$ nanocrystal, Yb^{3+} serves as a sensitizer that absorbs NIR light, and Er^{3+} or Tm^{3+} as activators that emit visible or NIR light. Full arrows indicate radiative transitions, dotted arrows indicate nonradiative energy transfer, and curled arrows indicate multiphonon relaxation. Adapted from Ref. [53] with permission.

Conventional organic fluorophores exhibit broad emission bands that may, for example, undergo shifts to longer or shorter wavelengths depending on the chemical environment. The emission lines of UCNPs, in contrast, are very narrow and do not shift because the electronic transitions relevant for the energy-transfer mechanism take place inside inner f-orbitals which are shielded from the environment. Consequently, the

line-like emissions of lanthanides allow a larger number and more stable codes to be generated in the visible spectrum than the broad and overlapping emission bands of organic fluorophores. These advantages of lanthanides were used earlier for designing (down-conversion) lanthanide-doped microbarcodes.[60] It should be noted, however, that the absolute emission intensities of UCNPs vary to some degree depending on their preparation, but these variations can be avoided by using only UCNPs from a single large-scale batch synthesis. Furthermore, the energy-transfer mechanism and the emission intensities of UCNPs are dependent on temperature, which has been exploited for the design of nanoscale thermometers.[61–63]

A third type of variation in the luminescence intensity of UCNPs arises from surface quenching effects.[64] Activator ions close to the surface come into contact with solvent molecules that can quench the emission. Water, in particular, exerts a strong quenching effect because of its high stretching vibrational energies that lead to nonradiative relaxation processes.[65] In Er^{3+}-doped UCNPs, for example, the vibrational modes of water (ca. 3500 cm^{-1}) closely match the energy difference for the transition between the $^4I_{11/2}$ to the $^4I_{13/2}$ state,[65] which is an intermediate for the emission of red light. Thus, the red emission of UCNPs is favored in water suspension. However, in general, the strong quenching effect of water results in the less-favorable situation that UCNPs are brighter in organic solvents than in water, but aqueous suspensions are the most relevant in a bioanalytical context. Heavy-metal ions and certain anions also can cause quenching.[66]

Generating smaller UCNPs usually leads to enhanced surface quenching effects because with decreasing radius the volume decreases more rapidly than the surface area. On the other hand, small UCNPs are required for many bioanalytical applications. An elegant way to minimize surface quenching effects and to maximize the upconversion efficiency is to grow a thin layer of host material ($NaYF_4$) without dopant ions on the surface of UCNPs.[67–69] A similar effect can be achieved by coating UCNPs with a silica shell.[70] Silica coatings confer additional advantages that will be discussed in Section 6.

3. Multicolor Tuning of UCNPs by the Material Composition

The modular assembly of sensitizers and activators in a common host lattice allows the generation of a combinatorial code of different colors. The dopant Yb^{3+} which has a single dominant energy transfer from $^2F_{7/2}$ to $^2F_{5/2}$ can be used to specifically absorb NIR light and to sensitize activator ions that display distinct emission lines. The kind of activator and its concentration in the $NaYF_4$ lattice allow the color to be tuned. However, the limitations of fluorometry have to be taken into account. As stated by Parker's law [Eq. (2)], the

$$F = I\,\varepsilon\,c\,l\,QY\,k \qquad (2)$$

measured fluorescence intensity F depends on a) the intensity of the excitation light I, b) the molar absorbance ε at the wavelength of excitation, c) the concentration of the luminophore (UCNP), d) the optical pathlength in the sample (l), e) the quantum yield (QY) of the luminophore, and f) various geometrical factors summarized as k.

It is even more difficult to standardize the nonlinear luminescence intensity of UCNPs because their quantum yield increases in a power-dependent manner.[71–74] For example, the two emission lines of Er^{3+}-doped UCNPs can each exhibit a different power dependence with increasing intensities of excitation light. It was observed that the green emission of Er^{3+} increases with the power of 2.0 and the red emission increases with the power of 2.4 of the excitation light intensity.[75] This effect, however, is only relevant if the excitation energy varies to a large extent.

One way to account for varying excitation intensities uses an internal reference signal. In this case, the host lattice is doped with two or more activator ions. The first activator ion provides a constant reference signal, while the second activator ion yields an encoding signal. To demonstrate this ratiometric encoding strategy, we have used UCNPs of type $NaYF_4$:Yb,Tm,Er, where Yb^{3+} serves as a sensitizer, Tm^{3+} as the activator for the constant reference signal (the blue emission), and Er^{3+} as the activator for the tunable encoding signal (the green and red emissions; see Figure 4).[76] The emission of Er^{3+} is the preferred encoding signal because its intensity is higher and hence can be tuned over a wider range than the intensity of the blue emission of Tm^{3+} at the optimal dopant concentration of 0.5%. The dopant concentration of

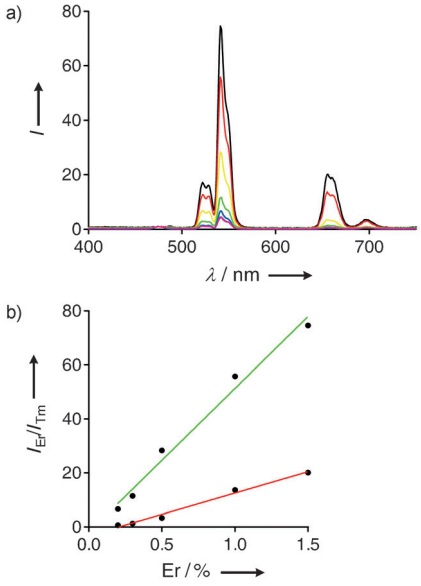

Figure 4. a) Tuning the intensity of individual emission lines by doping UCNPs of type $NaYF_4$:Yb,Er,Tm with various concentrations of the activator ion Er^{3+}. While the concentration of Tm^{3+} is kept constant to obtain a constant reference signal, the concentration of Er^{3+} is gradually increased from 0.01% (purple line) to 1.5% (black line) to increase the intensity of the green and red emission. The spectra are normalized with respect to the blue emission line of Tm^{3+} at 475 nm. b) A linear function is obtained for both the green and the red emission (indicated in the respective colors) by plotting the normalized signal intensities (I_{Er}/I_{Tm}) against the concentration of Er^{3+}.

Er^{3+} was gradually increased from 0.01% to 1.5% to obtain a set of seven codes.

In the case of ratiometric encoding, the absolute signal intensity i in Equation (1) is replaced by the ratio of I_{code} to I_{ref}. The number of analytical wavelengths (w) can be defined by choosing different activator ions (ai). Considering that one activator ion is required for the constant reference signal that has to be distinguishable from the background, the coding capacity of UCNPs can be expressed by Equation (3).

$$C_{UCNP} = \left(\frac{I_{code}}{I_{ref}}\right)^{(ai-1)} \quad (3)$$

The narrow emission lines of UCNPs allow many more codes to be accommodated in the visible than is possible with the broad emission bands of conventional organic fluorophores. In practice, the number of emission lines of UCNPs suitable for encoding is limited because the emission arises from transitions between discrete energy levels. However, the commonly used emission lines of Er^{3+}, Tm^{3+}, and Ho^{3+} are sufficient to obtain a large set of codes. A look at the combined color output of all the emission lines reveals that a continuous spectrum of visible light can be obtained (Figure 5).[77] Recently, a new energy migration mechanism in core–shell UCNPs was described that incorporates Tb^{3+}, Eu^{3+}, Dy^{3+}, and Sm^{3+} as activator ions.[78] Their additional emission lines further increase the encoding capacity of UCNPs.

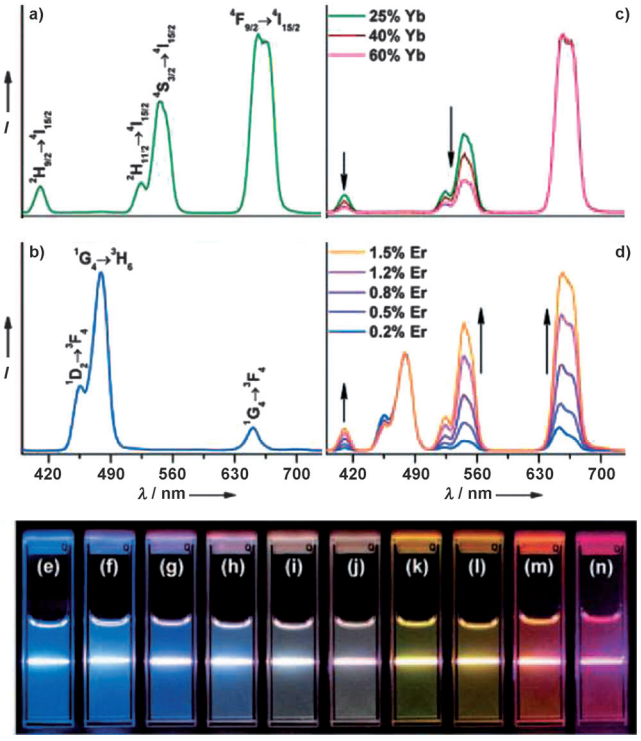

Figure 5. Emission spectra of UCNPs in ethanol under excitation at 980 nm : a) $NaYF_4$: 18% Yb^{3+}, 2% Er^{3+}, b) $NaYF_4$: 20% Yb^{3+}, 0.2% Tm^{3+}, c) $NaYF_4$: 25–60% Yb^{3+}, 2% Er^{3+}, and d) $NaYF_4$: 20% Yb^{3+}, 0.2% Tm^{3+}, 0.2–1.5% Er^{3+}. Photographs show the overall emission of UCNPs: e) $NaYF_4$: 20% Yb^{3+}, 0.2% Tm^{3+}, f–j) $NaYF_4$: 20% Yb^{3+}, 0.2% Tm^{3+}, 0.2–1.5 Er^{3+}, and k–n) $NaYF_4$: 18–60% Yb^{3+}, 2% Er^{3+}. Reprinted from Ref. [77] with permission. Copyright 2008 American Chemical Society.

Instead of incrementally increasing the intensity of the encoding signal, the complex signature of the multiple UCNP emission may be used as a "barcode". Each dopant composition would thus define a unique barcode. This encoding strategy was first developed for multiplexed bioanalysis by the group of Nann.[79] Silica-coated UCNPs of 20 nm diameter were doped with different activator ions to obtain the following set of four barcodes: a) $NaYF_4$:Yb for blue, green, red, and IR light, b) $NaYbF_4$:Er for green and red light, c) $NaYbF_4$:Tm for blue and NIR light, and d) $NaYbF_4$:Ho for green light. Even if mixed, all four were readily distinguishable. This barcoding system is robust but the number of codes is ultimately restricted by the number of available activator ions. More barcodes can be generated if different activator ions, each with a unique signature of multiple emission lines, are varied relative to each other in a way similar to ratiometric encoding. In this case, the relative intensities of the signatures define the code.

Not only the signature as a whole can be modulated, but also the multiple emission intensity of a single activator ion can be tuned individually by varying the temperature during synthesis,[80,81] the reaction solvent,[82] or by adding co-dopants such as Ce^{3+},[83] Dy^{3+},[84] or alkali ions.[85] The use of $KMnF_3$ instead of KYF_4 as a host lattice for Yb/Er results in UCNPs displaying a single emission line only.[86] Thus, the signatures can be modulated in a flexible way to obtain a large set of unique barcodes. For example, the groups of Zhang and Stucky[87] prepared core–shell UCNPs with a tunable core material for barcoding. The core consisted of a $NaYF_4$ host lattice doped with various combinations of Yb^{3+}, Ho^{3+}, Tm^{3+}, while the shell consisted of pure $NaYF_4$. Such particles ($NaYF_4$:Yb,Ho,Tm@$NaYF_4$) yielded ten distinguishable signatures. A model DNA hybridization assay was employed to demonstrate that the characteristic signatures of these UCNPs can be used as barcodes. Additionally, UCNPs consisting of lanthanide-doped oxides were used as barcodes for immunoassays.[88]

Multiplexed assays, such as flow cytometry or femtoliter arrays, rely on microspheres that have an approximately 100-fold larger diameter than UCNPs. As long as their emission lines can be spectrally resolved, two or more encoded UCNPs can be integrated in a single microsphere to define an exponentially increasing number of codes. While polymer microspheres, conventionally, are loaded with organic fluorophores[25] or quantum dots[26] to adjust the signal intensity of each type of microsphere, the accurate quantitative loading of the dye can be challenging. In contrast, the ratiometric codes of UCNPs loaded onto microspheres are not affected by the loading efficiency. This principle was recently demonstrated by using lanthanide-doped downconverting nanoparticles.[89] An automated microfluidic device was used to mix various amounts of either Dy^{3+}- or Sm^{3+}-doped luminescent nanoparticles with a constant amount of a reference Eu^{3+}-doped nanoparticle suspended in a PEG-diacrylate monomer. After photopolymerization, hydrophilic PEG-acrylate polymer microspheres of uniform size were obtained that carried 24 different ratiometric codes (Figure 6). These codes could

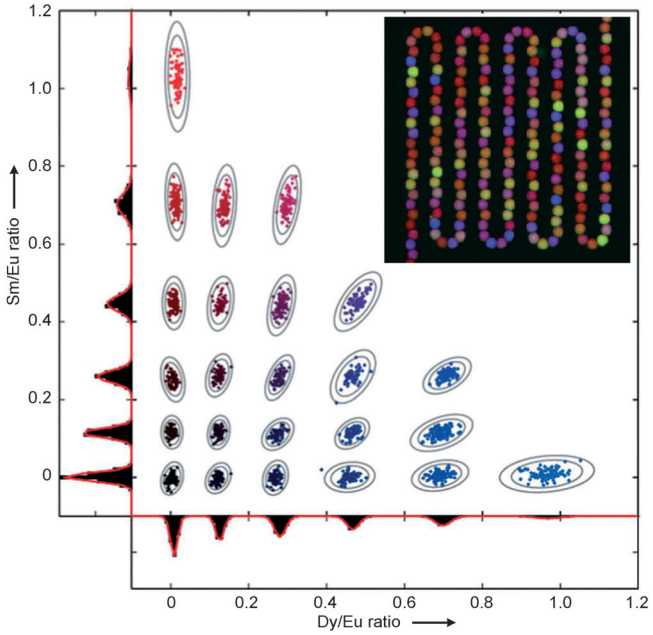

Figure 6. Matrix of encoded polymer microspheres. Crystalline YVO_4 nanoparticles were doped with either Dy^{3+} relative to Eu^{3+} or Sm^{3+} relative to Eu^{3+}. Both types of downconverting nanoparticles were integrated in a microsphere, and each point of the scatter plot represents one microsphere. Each type of encoded microsphere is clustered and well separated from microspheres that carry a different code. The intensity ratios of either the Dy^{3+} and Eu^{3+} emission or the Sm^{3+} and Eu^{3+} emission are shown as histograms along each axis. The histograms group all the codes together. The inset shows microspheres carrying different codes (indicated in "pseudocolors") in a microfluidic channel. Adapted from Ref. [89] with permission. Copyright 2012 The Royal Society of Chemistry.

be distinguished from each other with an error rate of less than 0.1%. This method can be easily adapted to generate upconversion codes for future applications.

4. Multicolor Tuning of UCNPs by an Optical Surface Layer

Rather than changing the composition of the upconverting material, the surface of the UCNPs can also be modulated with an optical-screening layer capable of filtering off certain emission lines. This strategy is particularly effective for UCNPs displaying two main emissions, such as $NaYF_4$:Yb,Er (green and red) or $NaYF_4$:Yb,Tm (blue and NIR). One of the dual emission lines can be reabsorbed selectively by adjusting the amount of an organic dye[90] or of gold nanoparticles[91] contained in the screen layer. The second emission is not reabsorbed and can serve as a reference signal. For example, the green emission line of UCNPs of type $NaYF_4$:Yb,Er was adjusted in ten increments by coating the nanoparticles with varying quantities of the purple dye rhodamine B. Each intensity level was then used to define a code (I_{code}; Figure 7a). As the absorption spectrum of rhodamine B does not display any overlap with the red emission line, the intensity of the red emission served as a constant reference signal (I_{ref}).

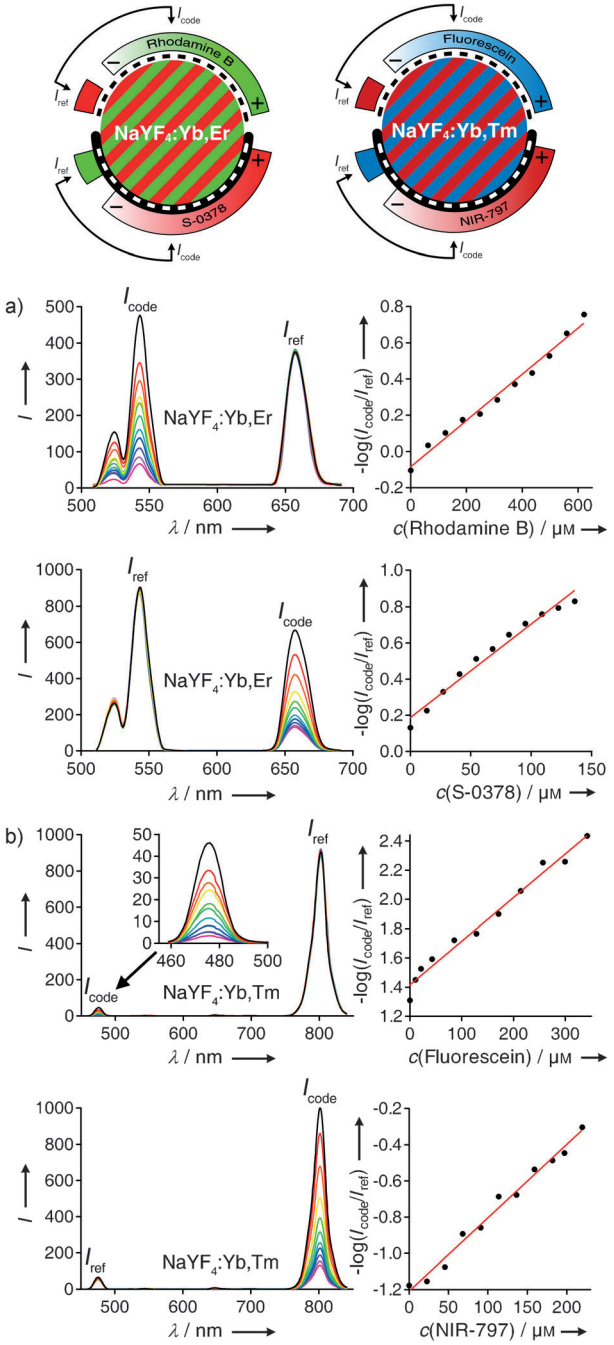

Figure 7. Tuning the emission intensity of UCNPs differentially by an organic dye. a) UCNPs of type $NaYF_4$:Yb,Er are covered with various concentrations of either rhodamine B (left) or the dye S-0378 (right). The concentration of rhodamine B is adjusted in ten increments to selectively reabsorb the green ($\lambda_{max} = 543$ nm) emission while the red ($\lambda_{max} = 657$ nm) emission remains constant. A linear function is obtained by plotting $-\log(I_{code}/I_{ref})$ against the concentration of rhodamine B. Alternatively, the intensity of the NIR emission can be selectively tuned by the dye S-0378. b) UCNPs of type $NaYF_4$:Yb,Tm display dual emission lines that can be adjusted individually either by fluorescein for the blue emission line ($\lambda_{max} = 475$ nm) or by the dye NIR-797 for the NIR emission line ($\lambda_{max} = 802$ nm). Adapted from Ref. [90] with permission.

The absorption of rhodamine B on the surface of UCNPs can be described [Eq. (4)] by analogy to the law of Lambert–Beer.

$$-\log\left(\frac{I_c}{I_0}\right) = ac \tag{4}$$

For a single (green) emission line of the UCNP—I_0 denotes the intensity of the unfiltered emission and I_c the emission intensity filtered by a given concentration (c) of rhodamine B on the nanoparticle's surface. The absorption (a) by rhodamine B depends on the wavelength λ, the thickness of the surface layer, and the microenvironment. If, however, the constant red emission of the UCNP is used as an internal reference signal for the filtered green emission, Equation (4) changes to Equation (5)

$$-\log\left(\frac{I_{code}}{I_{ref}}\right) = ac \tag{5}$$

where I_{ref} is the intensity of the unfiltered red emission and I_{code} is the intensity of the filtered green emission. A set of ten ratiometric codes was derived from the linear function $-\log(I_{code}/I_{ref})$. The encoding signal and the reference signal are interchangeable: If the screen layer consists of a blue–green dye rather than the purple dye rhodamine B, the red emission is selectively reabsorbed to modulate the encoding signal (I_{code}), while the green emission serves as a reference (I_{ref}). UCNPs of type $NaYF_4$:Yb,Tm (Figure 7b) display mainly blue and NIR emission lines that are well separated and whose intensities can be tuned individually by a screening layer possessing overlapping absorption spectra. For example, fluorescein was used to screen off the blue emission selectively, while a long-wavelength absorbing dye[45] was employed to screen off the emission in the NIR. In both cases, the unfiltered second emission served as an internal reference signal to yield ratiometric codes.

The dual emission lines of UCNPs type $NaYF_4$:Yb,Er display approximately the same intensity, but the NIR emission of $NaYF_4$:Yb,Tm is about 25-fold more intense than the blue one. In such cases, it is better to adjust the strong NIR emission by the screening dye and to use the blue emission as the reference signal. This avoids the detection of rather weak signals resulting from screening off the already weak blue emission.

In addition to their filter function for the emission of UCNPs, organic dyes also can serve as an extra coding element. For example, Li et al.[92] covered UCNPs of type $NaYF_4$:Yb,Er/Tm with a thin silica shell containing fluorophores or quantum dots. In this case, the UCNPs served as an energy donor for luminescence resonance energy transfer (LRET) to fluorescein, tetramethylrhodamine, or quantum dots. The emission spectrum of these core–shell nanoparticles changed because the original luminescence of UCNPs was quenched and new emission lines appeared that are characteristic for the dye in the silica layer. The combinatorial emission lines can be used as distinct barcodes. A similar approach was recently reported for in vivo imaging.[93] Furthermore, the dyes may be directly excited by visible light as in established bead encoding strategies.[25] Hence, two spectral signatures can be generated, one by visible light excitation, the other by NIR excitation leading to upconversion. Recently, an organic dye was used as an antenna for UCNPs that absorbed a broad band of NIR light and strongly enhanced the upconversion efficiency.[94] Modulating antenna dyes on UCNPs provides an additional way for encoding. Combining all these features as encoding parameters will expand the number of possible codes exponentially.

5. Multiparameter Encoding

The intensity of the multiple emission lines is not the only parameter of UCNPs suitable for ratiometric multiplexed encoding. The luminescence lifetime can be fairly easily determined using modern instrumentation and represents an attractive additional parameter in multiplexing, because the lifetime [unlike intensity; see the Parker law Eq. (2)] neither depends on the intensity of the excitation light nor on the sensitivity of the detector. Hence, it is an intrinsically self-referenced parameter.[95] Organic fluorophores and quantum dots usually have short lifetimes (on the order of 0.1 to 20 ns) that are more difficult to determine than longer lifetimes.[28] UCNPs, by contrast, have long-lived metastable states with decay times on the order of μs to several ms because f–f transitions of electrons are forbidden for symmetry reasons and therefore less likely.[57,96]

The long decay times of UCNPs can be efficiently separated from the short-lived autofluorescence of biological materials by using time-gated measurements. Downconverting nanoparticles of type $NaYF_4$:Ce,Tb, which can be sensitized by UV light and emit visible light, were used for time-resolved LRET to enable background-free biosensing (Figure 8).[97,98] It is, however, not necessary to separate background signals by time-resolved measurements when using UCNPs because their excitation by NIR light does not lead to autofluorescence in the first place. Rather, the wide range of lifetimes that are specific for each kind of UCNP represents a large set of multiparameter signatures and provides a new dimension for encoding that goes far beyond luminescence-intensity-based encoding.

The second approach for multiparametric encoding relies on a combination of UCNPs with other materials to design hybrid nanoparticles having additional properties, such as magnetism. Magnetic UCNPs can be separated by magnetic force[99] or serve as a contrast agent in magnetic resonance imaging (MRI).[100] Two types of magnetic UCNPs have been described: Superparamagnetism results if ferromagnetic bulk materials, such as iron oxide (ferrite; Fe_3O_4), fall below a critical size on the nanoscale. Unlike the bulk material, superparamagnetic nanoparticles do not have a permanent magnetic moment but are only magnetic as long as an external magnetic field is applied. This reversibility is important to avoid nanoparticle aggregation. Superparamagnetic UCNPs have been prepared by growing a luminescent $NaYF_4$:Yb,Er shell around an Fe_3O_4 core,[101] encapsulating UCNP with Fe_3O_4 in a silica shell,[102] or by conjugating superparamagnetic nanoparticles to the surface of UCNPs.[103,104]

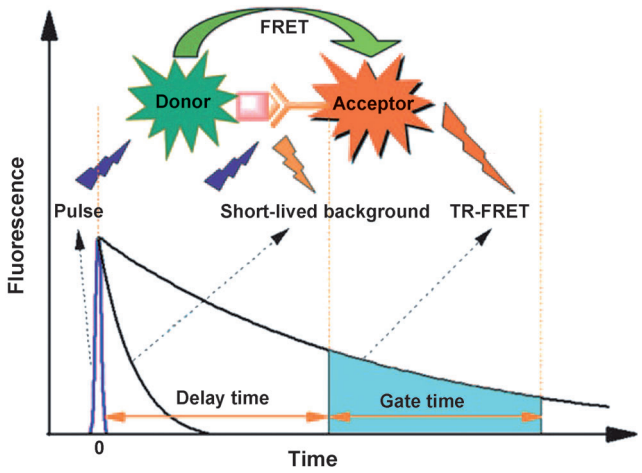

Figure 8. The principle of luminescent biosensing based on time-resolved LRET—more commonly referred to as fluorescence resonance energy transfer (FRET). The energy transfer from a downconversion nanoparticle of type $NaYF_4$:Ce,Tb apparently lengthens the luminescence lifetime of the short-lived organic dye bound to the nanoparticle surface. The time-resolved LRET signal can be measured by setting an appropriate delay and gate time. Reprinted from Ref. [97] with permission.

Paramagnetic materials are widely employed in MRI.[105] Gadolinium(III) is the most efficient contrast agent because it has the highest number of unpaired electrons (seven) and its long relaxation times increase the relaxation rate of surrounding ^1H nuclei in water.[106] Paramagnetic contrast agents are only effective in direct contact with water, so that they typically are applied in the form of chelates.[106] Following this scheme, paramagnetic hybrid nanoparticles were prepared by conjugating Gd^{3+}-chelates to the surface of UCNPs.[107] All lanthanide ions have similar atomic radii, and Gd^{3+} therefore can be integrated as a co-dopant into $NaYF_4$ nanocrystals. For example, Gd^{3+}-doping was used to control the size of UCNPs[108,109] or for sensitizing downconversion nanoparticles with UV light.[110] In fact, the paramagnetic properties of the co-dopant Gd^{3+} allowed the growth of UCNPs to be analyzed by magnetic resonance spectroscopy.[111]

Paramagnetic UCNPs doped with Gd^{3+} provide an additional dimension for multimodal imaging.[112] Hyeon et al.[100] gradually increased the concentration of Gd^{3+} in $NaYF_4$ nanocrystals from 0 to 12.8 mM to modulate the MRI signal in seven increments. After incubating cells with these paramagnetic UCNPs, the contrast in MRI was strongly increased. The group of Prasad[113] co-doped $NaYF_4$ nanocrystals with ion concentrations of 0, 2, 5, and 10 mM of Gd^{3+} and found a linear relationship between the Gd^{3+} concentration and the contrast enhancement. This relationship is analogous to the linear dependency of the luminescence signal on the concentration of the activator ion Er^{3+} (Figure 4). Consequently, the widely tunable magnetic resonance signal in our opinion represents a promising new encoding dimension. Another type of bimodal imaging probe was designed by combining the upconversion detection scheme with X-ray computed tomography (CT). In this case, either the co-dopant Yb^{3+} contained in UCNPs[114] or iodine attached to the surface of UCNPs served as a CT contrast agent.[115] Even trimodal hybrid particles were prepared, by modifying the luminescent $NaYF_4$:Yb,Er core with Gd^{3+} as a MRI contrast agent and ^{18}F as a radioactive isotope for emission tomography.[116] The modular assembly of UCNPs leaves ample room for incorporating new material features that will enable multiparametric encoding for very-high-throughput screening.

6. Synthesis and Surface Modification of Biocompatible UCNPs

Bioanalytical applications require the availability of UCNPs that are small, dispersible in water, nontoxic, amenable to (stable) surface functionalization, and displaying high upconversion efficiency. The optimization of theses parameters is still being researched, and presently no UCNPs are available that meet all these requirements.[117] Synthetic routes for various UCNPs have been reviewed elsewhere.[41–43] Bright UCNPs based on a $NaYF_4$ host lattice have been prepared by co-precipitation of lanthanide salts,[53,118] thermal decomposition of lanthanide trifluoroacetates,[119,120] solvothermal,[54,121,122] hydrothermal,[121,123] or ionothermal syntheses.[124] The solvothermal synthesis in oleic acid and octadecene has recently emerged as a preferred synthetic route because it is simple and yields highly monodisperse nanoparticles, no toxic by-products are generated, and no additional heating step is required to obtain the most efficient hexagonal phase. Cellular imaging requires particularly small UCNPs (under 10 nm in diameter) to allow for free access to intracellular compartments and a better clearance.[125] It has been challenging, however, to generate UCNPs that are both small and display high upconversion efficiency because of the various quenching effects discussed in Section 2. Only recently has it become possible to decrease the diameter of UCNP to below 10 nm by including different co-dopant ions, such as Yb^{3+}[126] or Gd^{3+},[108,127] into the host matrix, or by adding oleylamine to the reaction mixture.[109,128]

The solvothermal synthesis in oleic acid, yields UCNPs that are covered with a layer of oleic acid. Such particles are only dispersible in organic solvents and have to be further modified before they can be used in aqueous solutions.[42] Surface modification also is required for subsequent bioconjugation steps.[129] UCNPs have been made dispersible in water and amenable to bioconjugation either by replacing or modifying the oleic acid or by silanization. Oleic acid or other hydrophobic ligands on the surface of UCNPs can be replaced by ligand exchange with small hydrophilic ligands such as hydroxyethyldiphosphonic acid,[130] adipic acid,[131] citric acid,[75] or polymers.[65,132–135] Alternatively, amphiphilic block copolymers[68,136] or phospholipids[137] can be adsorbed to the surface layer of oleic acid by hydrophobic interactions. Oleic acid can be specifically oxidized at its unsaturated carbon–carbon bond by a Lemieux–von Rudloff reagent[138] or ozonolysis[104] to obtain azelaic acid on the nanoparticle surface. Finally, the surface coat can be removed from the UCNPs by protonating the oleic acid at pH 4.[139] The fact that the oleic acid on UCNPs can be stripped off under slightly acidic conditions already points to the major drawback of

ligand exchange or modification: the limited stability (and thus shelf life) arising from ligand dissociation or ligand exchange.[55] Additionally, polymers used for ligand exchange may lead to crosslinking and aggregation of nanoparticles.

A stable silica shell deposited on UCNPs makes them dispersible in water, biocompatible,[140] and renders the introduction of reactive groups and subsequent bioconjugation. Water-in-oil microemulsions are typically employed to grow a silica shell on the surface of oleic acid-coated UCNPs.[141] Hydrophobic UCNPs can be dispersed in an excess of cyclohexane containing a surfactant and aqueous ammonia. The thickness of the silica coating is adjusted by adding defined concentrations of tetraethyl orthosilicate and a further organosilane allows for the introduction of functional groups on the nanoparticle surface. Most commonly, reactive aminosilanes are employed to generate amino functionalized UCNPs[142,143] that can be conjugated to biomolecules such as biotin,[143] folic acid,[144,145] peptides,[146] avidin,[147,148] antibodies,[149,150] and DNA.[151,152] Silanization with 3-azidopropyltriethoxysilane enables click chemistry to be carried out on the nanoparticle,[153] for example, for DNA conjugation.[154] PEG-based silanization reagents have been used to introduce maleimide groups that allow for protein binding.[55]

The efficient and reproducible synthesis and surface modification of UCNPs provides the foundation for numerous bioanalytical applications in bioimaging and biosensing. The next Sections present selected examples of bioimaging and biosensing and highlight how they will benefit from the multiplexing capabilities of UCNPs.

7. Multicolor-Labeling of Cells with UCNPs for Bioimaging

Fluorescence imaging—in addition to MRI—is a powerful method for acquiring a detailed view inside living cells and organisms. Fluorescence makes species visible that display no MRI signals (such as oxygen and many ions), or whose signals cannot be differentiated from other species (such as fructose in presence of glucose). The quality of fluorescence bioimaging has been strongly improved by confocal, two-photon, or superresolution microscopy. As these techniques evolve, also the demands on fluorescent probes increase. For example, high excitation powers used in laser-induced fluorescence microscopy lead to strong photobleaching of conventional fluorophores.

UCNPs are a valuable alternative for bioimaging[155] because they do not photobleach at all. NIR light penetrates deeply into multilayered biological specimen so that using UCNPs of type $NaYF_4$:Yb,Er imaging of a rat body to a depth of 10 mm has been described.[156] It must be kept in mind, however, that not only the NIR light has to pass through tissue, but that the emission of the UCNPs in the visible also has to pass through the tissue to become detectable. Deep imaging has been achieved by employing UCNPs of type $NaYF_4$:Yb,Tm that emit NIR light at $\lambda = 800$ nm.[157,158] The group of Andersson-Engels[72] has recently demonstrated that the nonlinearly power-dependent NIR emission of Tm-doped UCNPs enables high-resolution imaging. The deep penetration range of NIR light in biological tissues has also been exploited to activate photocaged compounds[159–163] or to induce the generation of reactive oxygen species for photodynamic therapy[164–166] in deep tissues by using UCNPs that emit short-wavelength light.

Unmodified UCNPs were first used to monitor the biodistribution in nematode worms,[167–169] higher animals,[140,156,170] and plants.[171] The advantages of UCNPs were then exploited for biomedical research in whole animals, and reviewed recently.[172] Specific ligands on the surface of UCNPs are not required in case of vascular and lymphatic imaging[74,173,174] or cell tracking. Multiplexed cell-tracking experiments were performed by labeling different cell lines with encoded UCNPs. The group of Liu[175] encoded UCNPs by varying the material composition: Three codes were generated by using two types of UCNPs doped with different fractions of Er^{3+} and one type of Tm^{3+}-doped UCNP.

UCNPs are readily internalized by endocytosis, especially if they are modified with amino groups.[176] Encoded cells also may be injected into animals to track cellular dynamics over time. The group of Wang[177] co-doped upconverting nanorods of type $NaYF_4$:Yb,Er with La^{3+} or Ce^{3+} to tune the emission intensities. They also noted that the color output shifts from green to red if UCNPs are located in deeper tissues because red light can cross larger distances through biological materials. On the one hand, this emission shift can serve to estimate the location of UCNPs under the skin. In this case, however, it is difficult to implement an encoding strategy based on the emission intensity of UCNPs. Even a ratiometric approach is hindered because the ratio of the two emission lines shifts as the location of the UCNPs is changed. Kim's group[178] used combinations of UCNPs and quantum dots for dual labeling of cells and tracking them in animal models (Figure 9). While encoding strategies based on the material composition are more abundant, UCNPs encoded by different surface layers of organic dyes were also used to track cells in vivo.[93]

Although the cellular uptake and cytotoxicity of UCNPs can be studied without specific surface ligands,[75,100,179–182] the targeting of cancer specific structures requires the attachment of ligands. Coating UCNPs with folic acid directs them to the folic acid receptor,[144,183] which is overexpressed on many tumor cells.[184] Alternatively, UCNPs have been labeled with neurotoxins[185] or a cyclic peptide (RGDFK) specific for the $\alpha_v\beta_3$ integrin ligand on the surface of certain tumor cells.[146,186] The most studies by far on cancer cell targeting relate to coating the surface of UCNPs with tumor-specific antibodies.[113,150,187–190] Without using an encoding strategy, only one of many tumor markers can be investigated per experiment. Labeling different ligands with encoding UCNPs, in contrast, would allow different tumor markers to be monitored simultaneously.

In addition to cell labeling, it is feasible to design specific molecular probes ("sensors") that change their luminescence in presence of an intracellular analyte, such as oxygen.[191] Numerous responsive organic fluorophores are available and have recently been reviewed.[192] The design of such UCNP-derived probes, however, is quite challenging because they

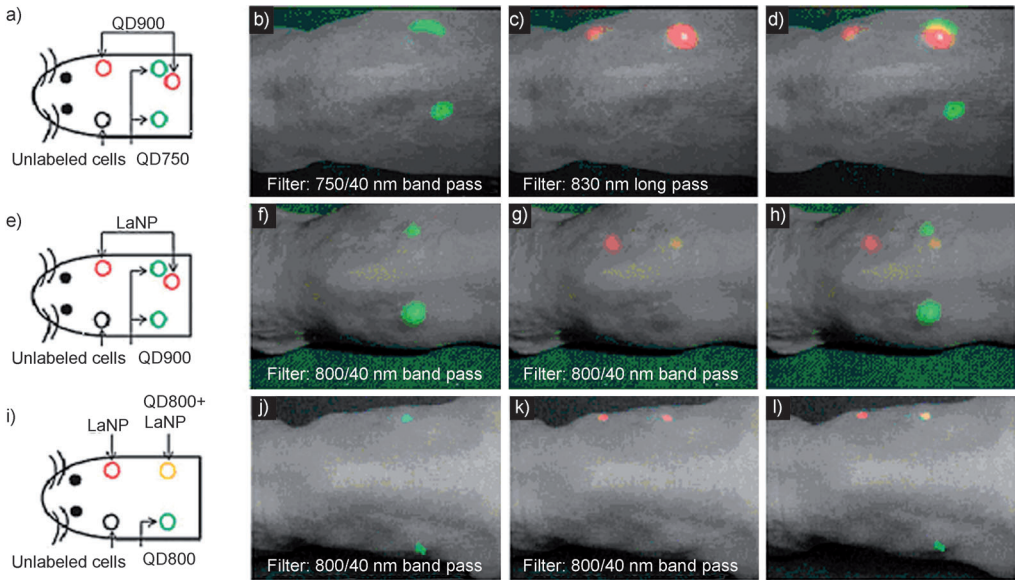

Figure 9. HeLa cells labeled with different types of quantum dots or UCNPs of type $NaYF_4$:Yb^{3+},Tm^{3+} are injected subcutaneously into hairless mice. a) Scheme of the implantation experiment using cells labeled with QD750 (green) and QD900 (red) quantum dots. The mouse in (b) and (c) is illuminated with a 660 nm laser. d) Merged image of (b) and (c). e) Implantation experiment using cells labeled with QD800 (green) and UCNP (red). f) Image of the subject illuminated using a 660 nm laser; g) image of the subject excited using a 980 nm diode laser. h) Merged image of (f) and (g). i) Scheme of the QD800- and UCNP-labeled cell co-incubation implantation experiment: HeLa cells are labeled with QD800 (green), UCNP (red), both QD800 and UCNP (yellow). j) Image under 660 nm laser excitation and k) image under 980 nm laser excitation. l) Merged image of (j) and (k). Reprinted from Ref. [178] with permission. Copyright 2011 The Royal Society of Chemistry.

usually do not respond to their chemical environment. In fact, their inertness is most welcome in many situations. The only parameters that directly affect the luminescence of UCNPs are temperature[62,63,193,194] and—with some limitations—pH value,[139] and some heavy-metal quenchers.[66] The detection of almost any other intracellular analyte requires the surface of UCNPs to be modified, for example, with an analyte-specific organic dye that is excited by the emission light of UCNPs.[92] The multicolor emission of UCNPs is beneficial for intracellular sensing because one emission line provides a fairly constant reference signal, whereas a second one is modulated by the analyte of interest through the organic probe on the surface of the UCNP. This strategy offers many options for new luminescent probes in intracellular applications.

8. Spatially Encoded Heterogeneous Bioassays

The weak interaction of NIR light with biological materials is the major driving force behind the design of biological assays based on the upconversion technology.[195] Before nanosized UCNPs became available, the group of Tanke[196] had already pioneered the use of sub-micrometer-sized (0.1–1 μm) upconverting particles in histology and heterogeneous bioassays. The detection limit of DNA hybridization on a microarray could be decreased by a factor of four when the upconversion technology instead of a conventional fluorolabeling was applied.[197]

Such upconverting particles also were employed in lateral flow assays (LFAs) for the detection of DNA,[198,199] pathogens,[200,201] and proteins.[202] In a typical LFA, the analyte in a sample binds to a detection reagent (such as an antibody) and then flows across a nitrocellulose membrane that contains test lines with an immobilized capture antibody specific for the analyte. Additionally, a second capture antibody specific for the detection reagent is immobilized on a control line to check for the assay performance. The pregnancy test is probably the best-known LFA and enables the detection of the pregnancy hormone human chorionic gonadotropin (hCG) in urine. Compared to the conventionally used colloidal gold or latex particles, the detection sensitivity of hCG in LFSs was improved by a factor of 10 to 100 when using upconverting particles.[203] LFAs also are amenable to multiplexing. It was shown[203] that, in addition to hCG, two more proteins were detectable in an LFA on the same strip. The upconverting microparticles contained different dopants to assign a distinct color to each analyte. In an example of a competitive LFA, twelve separate test lines on a nitrocellulose membrane were used to detect several drugs in saliva simultaneously.[204] To further enhance the degree of multiplexing, two types of upconverting microparticles, each with a distinct dopant composition and color, were employed for different analytes. This LFA was used for the multiplexed detection of pathogens in saliva and plasma.[205] Antigens derived from HIV, hepatitis C, and tuberculosis were immobilized on separate test lines on a nitrocellulose membrane to capture respective antibodies that indicate the state of an infection.

The group of Soukka[206–208] applied submicrometer-sized upconverting particles for immunoassays in microtiter plates. They noted, however, that nonspecific binding of these relatively large particles compromises sensitivity, and they stressed the need for monodisperse nano- (rather than micro-)-particles. Indeed, by using UCNPs with oligonucleotide arrays immobilized on the surface of a microtiter plate, a much better assay performance was accomplished for the multiplexed detection and genotyping of human adenoviruses.[209]

9. Microsphere-Encoded Heterogeneous Bioassays

The microtiter plate as the solid support for an immunoassay can be replaced by microspheres, and microspheres in suspension can be sorted by flow cytometry or assembled into femtoliter arrays as described in the Introduction.[11] For the development of a sandwich immunoassay on a microsphere, proteins, viruses, bacteria, or even spores were immobilized on the surface of polystyrene or magnetic microspheres.[210] Then, a target-specific antibody labeled with a submicrometer-sized upconverting particle was added to the microspheres, and the labeled microspheres were sorted by flow cytometry. In another format, the analyte on the surface of the microsphere was detected by adding a biotinylated antibody, which was then detected by binding of neutravidin-labeled upconverting particles. For multiplexing, the microspheres were labeled with lanthanides that emit different colors.

While microsphere assays in principle allow for high-throughput screening and a high degree of multiplexing, in practice they are limited by the number of available identifier codes. Thus, the ability to generate a multitude of encoded UCNPs or to combine different types of UCNPs in one microsphere, as shown in Figure 6, would greatly advance the performance of microsphere assays. Even more importantly, the upconversion detection scheme can be completely reserved for encoding many microspheres, while a conventional fluorophore can be used as a reporter for analyte binding. In this case, the excitation modes of UCNPs and conventional fluorophores are well separated and there is no luminescent crosstalk.

10. Multiplexed Homogeneous Assays

In homogeneous assay formats, both the analyte and the detection reagents remain in solution.[211–213] For this kind of assay, it is required that the emission intensity of UCNPs is specifically modulated by an analyte. This modulation is most commonly achieved by luminescence resonance energy transfer (LRET), in which the UCNP serves as the donor and an organic dye,[214] gold nanoparticle,[149,215,216] quantum dot,[217] carbon nanoparticle,[218,219] graphene oxide,[220] manganese dioxide,[221] or phycobiliprotein[222] as the acceptor. Gold nanoparticles have been shown to be the most efficient acceptors for UCNPs (Figure 10) but their large size (compared to organic dyes) can lead to steric hindrance during analyte recognition.

LRET is a critically distance-dependent process,[223] and only emitter ions close to the surface of UCNPs can be quenched.[224] Thus, small UCNPs that are highly dispersible in water are beneficial for homogeneous assays. The quenching efficiency of organic dyes, however, typically is below 50% even though it has recently been raised to 82%.[225] To avoid the low quenching efficiency of upconversion LRET, a nuclease assay based on sequential energy transfer was implemented (Figure 11).[224]

The group of Wheeler[226] used UCNPs of the type $NaYF_4$:Yb,Er as a donor and a fluorescent dye as an acceptor for a homogeneous DNA assay. Single-stranded DNA was attached to amino-silanized UCNPs, and a complementary DNA strand was labeled with carboxyrhodamine whose excitation spectrum overlaps the green emission of the UCNPs. After hybridization with a complementary 26-mer oligonucleotide, the green emission of the UCNP was quenched. This method had a detection limit of as little as 1.3 nM DNA. The discrimination of single-nucleotide mismatches enabled the detection of point mutations associated with sickle-cell anemia.[227,228] Soukka's group[229] exploited the multiple emission lines of UCNPs for the multiplexed detection of DNA. Amino-functionalized UCNP of the type $NaYF_4$:Yb,Er were surface modified with two different capture DNA strands. After binding of single-stranded target DNA, two detection probes, specific for the target

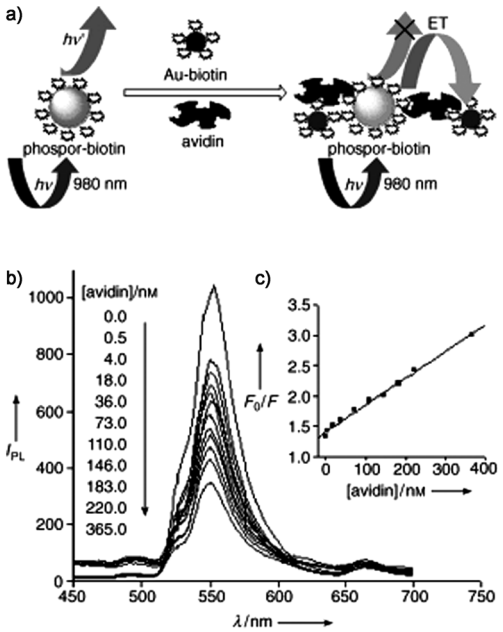

Figure 10. a) Scheme of an LRET-based assay for avidin. Biotinylated UCNPs serve as energy donors and biotinylated gold nanoparticles as energy acceptors. Avidin crosslinks donor and acceptor. b) Emission spectra in the presence of increasing avidin concentrations. c) A linear relationship between the relative luminescence intensity (F_0/F) and the concentration of avidin is observed. Reprinted from Ref. [215] with permission.

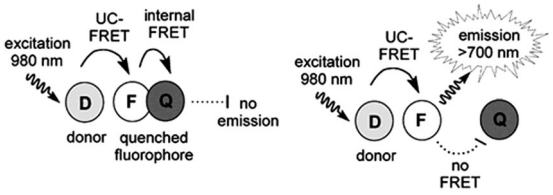

Figure 11. Homogeneous enzyme-activity assay consisting of a UCNP donor (D) and an internally quenched double-labeled substrate. The fluorophore is excited through upconversion luminescence resonance energy transfer (UC-FRET) under continuous NIR excitation. The intact substrate is not fluorescent. The hydrolytic enzyme separates the fluorophore (F) and quencher (Q) located at the opposite ends of the substrate so that the emission of the fluorophore is restored. Reprinted from Ref. [224] with permission.

DNA, were added that selectively absorb either the green or the red emission of the UCNPs, such that their emission could be detected separately. By using a single NIR excitation wavelength, it was possible to detect two different target DNA strands simultaneously without mutual interference.

There is a substantial research activity on the use of UCNPs in homogeneous assay formats. For example, homogeneous assays have been described for the background-free detection of hormones,[230] glucose,[216,220] lectins,[231] or ATP[232] in blood or other untreated biological samples. Substrates for nucleases or proteases typically consist of oligomeric nucleotide or peptide sequences, respectively[233] whose opposite ends are labeled with a FRET donor and acceptor. While the fluorescence is quenched in the intact oligonucleotide or peptide, enzymatic action separates the donor and acceptor and thereby restores the emission of the donor. As the fluorescent donor dye can be replaced by an UCNP, it is straightforward to apply the LRET upconversion technology to existing FRET substrates. This detection scheme was used to design assays for endonucleases,[224] caspases,[234] thrombin,[218] or metalloproteinases.[219]

11. Multiple Chemical Sensing

UCNPs incorporated into sensor films were employed for online and fully reversible monitoring of ammonia,[235] carbon dioxide,[236] oxygen,[237] pH value,[238] and heavy-metal ions.[66,239] The UCNPs themselves are inert but can serve as nanosized light sources whose emission is modulated by an added indicator probe. The screening or quenching effect of the nonfluorescent indicator depends on the concentration of the species to be sensed. The analyte-dependent reduction of the emission of UCNPs was applied to sensors for ammonia,[235] carbon dioxide,[236] and pH value.[238] Conceivably, the use of UCNPs of different emission colors may lead to sensors for multiple chemicals, but this has not been demonstrated to date. In another scheme, the UCNPs served as nanolamps capable of photoexciting a fluorescent probe that is quenched, for example, by oxygen.[237] The intensity and decay time of the emission of the probe is related to the local O_2 partial pressure. This method is also waiting to be extended to multiplexed (bio)sensing.

12. Summary and Outlook

Both multiplexed encoding and photon upconversion are emerging technologies with an enormous potential for bioanalytical applications. Multiplexed encoding lays the foundation for the quantitation of a large number of analytes in parallel. The number of possible codes can be calculated by Equation (1). Compared to conventional labels, UCNPs have many advantages: They can be excited with NIR light and emit visible light (anti-Stokes emission). NIR light penetrates biological materials much better and does not generate strong autofluorescence. The spectrum of UCNPs typically displays multiple and narrow emission lines which minimizes crosstalk between coding elements. The intensity of multiple emission lines can be either tuned individually for ratiometric encoding, but the whole spectral signature may also serve as a barcode. Unlike quantum dots, UCNPs do not contain toxic heavy-metal ions.

Three general strategies are feasible to design a large number of spectral codes based on UCNPs: First, the composition of the activator ions is modulated and used to define the emission spectrum or colors. Second, the emission is modulated by an added organic dye that usually is attached to the UCNP surface. Third, hybrid materials are used with additional features, such as magnetism. Each strategy on its own can be used to obtain a large set of codes. The number of possible codes, however, increases exponentially by combining these approaches. For example, five different types of UCNPs, each defining ten ratiometric codes, yield 100 000 (10^5) codes, while the number of codes increases to 10^{25} [$(10^5)^5$] when hybrid UCNPs are used that additionally have five paramagnetic intensity levels. This number should be enough for the foreseeable future of multiplexed analyte detection. The large encoding power of UCNPs even goes far beyond bioanalytical applications, for example, into areas such as security applications, anti-counterfeit, or the authentication of documents and commercial products.[240–242]

So why UCNPs are not more widely distributed, yet? One answer is that despite the tremendous advancement in the preparation of UCNPs there is still a lack of general methods for the preparation of bright and small hydrophilic UCNPs that are required for bioimaging and bioanalytical applications. Only recently, UCNPs have become commercially available. In our perception, UCNPs presently are at the stage that quantum dots were twenty years ago. While quantum dots are compatible with classical fluorescence instrumentation, the detection scheme for the anti-Stokes emission of UCNPs poses additional hurdles to their wider applicability. For example, microtiter plate readers and flow cytometers have to be specifically adapted to upconversion detection schemes. In fact, only a few fluorometers are commercially available that can be operated in the upconversion mode. The situation is somewhat better for fluorescence microscopy because many instruments originally developed for two-photon microscopy can also be used to work with UCNPs. We predict that, once these issues are resolved, UCNP-based encoding strategies will pave new ways in multiplexed genotyping, high-throughput screening, multiplexed cell targeting, point-of-care diagnosis,[243] and product authentication.

We thank Stefan Wilhelm for recording the TEM images shown in Figure 2 and Dr. Daniela E. Achatz for the data shown in Figure 4.

Received: October 11, 2013
Published online: February 28, 2013

[1] P. Hardenbol, F. L. Yu, J. Belmont, J. MacKenzie, C. Bruckner, T. Brundage, A. Boudreau, S. Chow, J. Eberle, A. Erbilgin, M. Falkowski, R. Fitzgerald, S. Ghose, O. Iartchouk, M. Jain, G. Karlin-Neumann, X. H. Lu, X. Miao, B. Moore, M. Moorhead, E. Namsaraev, S. Pasternak, E. Prakash, K. Tran, Z. Y. Wang,

H. B. Jones, R. W. Davis, T. D. Willis, R. A. Gibbs, *Genome Res.* **2005**, *15*, 269 – 275.
[2] J. M. Klostranec, Q. Xiang, G. A. Farcas, J. A. Lee, A. Rhee, E. I. Lafferty, S. D. Perrault, K. C. Kain, W. C. W. Chan, *Nano Lett.* **2007**, *7*, 2812 – 2818.
[3] M. Meldal, S. F. Christensen, *Angew. Chem.* **2010**, *122*, 3551 – 3554; *Angew. Chem. Int. Ed.* **2010**, *49*, 3473 – 3476.
[4] S. Ahn, D. M. Kulis, D. L. Erdner, D. M. Anderson, D. R. Walt, *Appl. Environ. Microbiol.* **2006**, *72*, 5742 – 5749.
[5] S. P. Fodor, J. L. Read, M. C. Pirrung, L. Stryer, A. T. Lu, D. Solas, *Science* **1991**, *251*, 767 – 773.
[6] N. H. Finkel, X. H. Lou, C. Y. Wang, L. He, *Anal. Chem.* **2004**, *76*, 352A – 359A.
[7] R. Wilson, A. R. Cossins, D. G. Spiller, *Angew. Chem.* **2006**, *118*, 6250 – 6263; *Angew. Chem. Int. Ed.* **2006**, *45*, 6104 – 6117.
[8] R. J. Fulton, R. L. McDade, P. L. Smith, L. J. Kienker, J. R. Kettman, *Clin. Chem.* **1997**, *43*, 1749 – 1756.
[9] E. Morgan, R. Varro, H. Sepulveda, J. A. Ember, J. Apgar, J. Wilson, L. Lowe, R. Chen, L. Shivraj, A. Agadir, R. Campos, D. Ernst, A. Gaur, *Clin. Immunol.* **2004**, *110*, 252 – 266.
[10] P. O. Krutzik, G. P. Nolan, *Nat. Methods* **2006**, *3*, 361 – 368.
[11] H. H. Gorris, D. R. Walt, *Angew. Chem.* **2010**, *122*, 3970 – 3986; *Angew. Chem. Int. Ed.* **2010**, *49*, 3880 – 3895.
[12] H. H. Gorris, T. M. Blicharz, D. R. Walt, *FEBS J.* **2007**, *274*, 5462 – 5470.
[13] S. R. Nicewarner-Pena, R. G. Freeman, B. D. Reiss, L. He, D. J. Pena, I. D. Walton, R. Cromer, C. D. Keating, M. J. Natan, *Science* **2001**, *294*, 137 – 141.
[14] K. Braeckmans, S. C. De Smedt, C. Roelant, M. Leblans, R. Pauwels, J. Demeester, *Nat. Mater.* **2003**, *2*, 169 – 173.
[15] D. C. Pregibon, M. Toner, P. S. Doyle, *Science* **2007**, *315*, 1393 – 1396.
[16] H. Lee, J. Kim, H. Kim, S. Kwon, *Nat. Mater.* **2010**, *9*, 745 – 749.
[17] S. C. Chapin, D. C. Appleyard, D. C. Pregibon, P. S. Doyle, *Angew. Chem.* **2011**, *123*, 2337 – 2341; *Angew. Chem. Int. Ed.* **2011**, *50*, 2289 – 2293.
[18] S. H. Kim, J. W. Shim, S. M. Yang, *Angew. Chem.* **2011**, *123*, 1203 – 1206; *Angew. Chem. Int. Ed.* **2011**, *50*, 1171 – 1174.
[19] H. Fenniri, L. H. Ding, A. E. Ribbe, Y. Zyrianov, *J. Am. Chem. Soc.* **2001**, *123*, 8151 – 8152.
[20] H. Fenniri, S. Chun, L. H. Ding, Y. Zyrianov, K. Hallenga, *J. Am. Chem. Soc.* **2003**, *125*, 10546 – 10560.
[21] J. Raez, D. R. Blais, Y. Zhang, R. A. Alvarez-Puebla, J. P. Bravo-Vasquez, J. P. Pezacki, H. Fenniri, *Langmuir* **2007**, *23*, 6482 – 6485.
[22] L. Sun, K. B. Sung, C. Dentinger, B. Lutz, L. Nguyen, J. W. Zhang, H. Y. Qin, M. Yamakawa, M. Q. Cao, Y. Lu, A. J. Chmura, J. Zhu, X. Su, A. A. Berlin, S. Chan, B. Knudsen, *Nano Lett.* **2007**, *7*, 351 – 356.
[23] J. H. Kim, H. Kang, S. Kim, B. H. Jun, T. Kang, J. Chae, S. Jeong, J. Kim, D. H. Jeong, Y. S. Lee, *Chem. Commun.* **2011**, *47*, 2306 – 2308.
[24] S. Lee, S. Joo, S. Park, S. Kim, H. C. Kim, T. D. Chung, *Electrophoresis* **2010**, *31*, 1623 – 1629.
[25] F. J. Steemers, J. A. Ferguson, D. R. Walt, *Nat. Biotechnol.* **2000**, *18*, 91 – 94.
[26] M. Y. Han, X. H. Gao, J. Z. Su, S. Nie, *Nat. Biotechnol.* **2001**, *19*, 631 – 635.
[27] L. Wang, W. H. Tan, *Nano Lett.* **2006**, *6*, 84 – 88.
[28] M. Grabolle, P. Kapusta, T. Nann, X. Shu, J. Ziegler, U. Resch-Genger, *Anal. Chem.* **2009**, *81*, 7807 – 7813.
[29] B. K. Oh, J. M. Nam, S. W. Lee, C. A. Mirkin, *Small* **2006**, *2*, 103 – 108.
[30] J. R. Epstein, J. A. Ferguson, K. H. Lee, D. R. Walt, *J. Am. Chem. Soc.* **2003**, *125*, 13753 – 13759.
[31] L. M. Liz-Marzán, *Langmuir* **2006**, *22*, 32 – 41.
[32] R. Bukasov, J. S. Shumaker-Parry, *Nano Lett.* **2007**, *7*, 1113 – 1118.
[33] M. A. El-Sayed, *Acc. Chem. Res.* **2001**, *34*, 257 – 264.
[34] S. J. Oldenburg, R. D. Averitt, S. L. Westcott, N. J. Halas, *Chem. Phys. Lett.* **1998**, *288*, 243 – 247.
[35] J. Pérez-Juste, I. Pastoriza-Santos, L. M. Liz-Marzán, P. Mulvaney, *Coord. Chem. Rev.* **2005**, *249*, 1870 – 1901.
[36] C. X. Yu, J. Irudayaraj, *Anal. Chem.* **2007**, *79*, 572 – 579.
[37] U. Resch-Genger, M. Grabolle, S. Cavaliere-Jaricot, R. Nitschke, T. Nann, *Nat. Methods* **2008**, *5*, 763 – 775.
[38] R. Gill, M. Zayats, I. Willner, *Angew. Chem.* **2008**, *120*, 7714 – 7736; *Angew. Chem. Int. Ed.* **2008**, *47*, 7602 – 7625.
[39] S. Giri, E. A. Sykes, T. L. Jennings, W. C. W. Chan, *ACS Nano* **2011**, *5*, 1580 – 1587.
[40] T. Song, Q. Zhang, C. L. Lu, X. Q. Gong, Q. H. Yang, Y. H. Li, J. Q. Liu, J. Chang, *J. Mater. Chem.* **2011**, *21*, 2169 – 2177.
[41] M. Haase, H. Schäfer, *Angew. Chem.* **2011**, *123*, 5928 – 5950; *Angew. Chem. Int. Ed.* **2011**, *50*, 5808 – 5829.
[42] F. Wang, X. G. Liu, *Chem. Soc. Rev.* **2009**, *38*, 976 – 989.
[43] H. S. Mader, P. Kele, S. M. Saleh, O. S. Wolfbeis, *Curr. Opin. Chem. Biol.* **2010**, *14*, 1 – 15.
[44] O. S. Wolfbeis in *Molecular luminescence spectroscopy: Methods and applications*, *Vol. 1* (Ed.: S. G. Schulman), Wiley, New York, **1985**, pp. 167 – 369.
[45] H. H. Gorris, S. M. Saleh, D. B. M. Groegel, S. Ernst, K. Reiner, H. Mustroph, O. S. Wolfbeis, *Bioconjugate Chem.* **2011**, *22*, 1433 – 1437.
[46] M. Albota, D. Beljonne, J. L. Bredas, J. E. Ehrlich, J. Y. Fu, A. A. Heikal, S. E. Hess, T. Kogej, M. D. Levin, S. R. Marder, D. McCord-Maughon, J. W. Perry, H. Rockel, M. Rumi, C. Subramaniam, W. W. Webb, X. L. Wu, C. Xu, *Science* **1998**, *281*, 1653 – 1656.
[47] D. R. Larson, W. R. Zipfel, R. M. Williams, S. W. Clark, M. P. Bruchez, F. W. Wise, W. W. Webb, *Science* **2003**, *300*, 1434 – 1436.
[48] G. S. He, L. S. Tan, Q. Zheng, P. N. Prasad, *Chem. Rev.* **2008**, *108*, 1245 – 1330.
[49] M. Pawlicki, H. A. Collins, R. G. Denning, H. L. Anderson, *Angew. Chem.* **2009**, *121*, 3292 – 3316; *Angew. Chem. Int. Ed.* **2009**, *48*, 3244 – 3266.
[50] P. Campagnola, *Anal. Chem.* **2011**, *83*, 3224 – 3231.
[51] F. Auzel, *Chem. Rev.* **2004**, *104*, 139 – 173.
[52] K. W. Krämer, D. Biner, G. Frei, H. U. Güdel, M. P. Hehlen, S. R. Lüthi, *Chem. Mater.* **2004**, *16*, 1244 – 1251.
[53] S. Heer, K. Kömpe, H. U. Güdel, M. Haase, *Adv. Mater.* **2004**, *16*, 2102 – 2105.
[54] Z. Q. Li, Y. Zhang, *Nanotechnology* **2008**, *19*, 345606.
[55] R. B. Liebherr, T. Soukka, O. S. Wolfbeis, H. H. Gorris, *Nanotechnology* **2012**, *23*, 485103.
[56] A. Aebischer, M. Hostettler, J. Hauser, K. Kramer, T. Weber, H. U. Güdel, H. B. Buergi, *Angew. Chem.* **2006**, *118*, 2869 – 2873; *Angew. Chem. Int. Ed.* **2006**, *45*, 2802 – 2806.
[57] J. F. Suyver, J. Grimm, M. K. van Veen, D. Biner, K. W. Kramer, H. U. Güdel, *J. Lumin.* **2006**, *117*, 1 – 12.
[58] J.-C. G. Bünzli, *Chem. Rev.* **2010**, *110*, 2729 – 2755.
[59] P. Hänninen, H. Härmä, *Springer Series on Fluorescence*, *Vol. 7* (Ed.: O. S. Wolfbeis), Springer, Heidelberg, **2011**, pp. 1 – 45.
[60] M. J. Dejneka, A. Streltsov, S. Pal, A. G. Frutos, C. L. Powell, K. Yost, P. K. Yuen, U. Muller, J. Lahiri, *Proc. Natl. Acad. Sci. USA* **2003**, *100*, 389 – 393.
[61] M. A. R. C. Alencar, G. S. Maciel, C. B. de Araujo, A. Patra, *Appl. Phys. Lett.* **2004**, *84*, 4753 – 4755.
[62] L. H. Fischer, G. S. Harms, O. S. Wolfbeis, *Angew. Chem.* **2011**, *123*, 4640 – 4645; *Angew. Chem. Int. Ed.* **2011**, *50*, 4546 – 4551.
[63] A. Sedlmeier, D. Achatz, L. H. Fischer, H. H. Gorris, O. S. Wolfbeis, *Nanoscale* **2012**, *4*, 7090 – 7096.

[64] F. Wang, J. A. Wang, X. G. Liu, *Angew. Chem.* **2010**, *122*, 7618 – 7622; *Angew. Chem. Int. Ed.* **2010**, *49*, 7456 – 7460.
[65] J. C. Boyer, M. P. Manseau, J. I. Murray, F. C. J. M. van Veggel, *Langmuir* **2010**, *26*, 1157 – 1164.
[66] S. M. Saleh, R. Ali, O. S. Wolfbeis, *Chem. Eur. J.* **2011**, *17*, 14611 – 14617.
[67] F. Vetrone, R. Naccache, V. Mahalingam, C. G. Morgan, J. A. Capobianco, *Adv. Funct. Mater.* **2009**, *19*, 2924 – 2929.
[68] G. S. Yi, G. M. Chow, *Chem. Mater.* **2007**, *19*, 341 – 343.
[69] H. Guo, Z. Q. Li, H. S. Qian, Y. Hu, I. N. Muhammad, *Nanotechnology* **2010**, *21*, 125602.
[70] Q. Lü, F. Y. Guo, L. Sun, A. H. Li, L. C. Zhao, *J. Appl. Phys.* **2008**, *103*, 123533.
[71] C. Würth, J. Pauli, C. Lochmann, M. Spieles, U. Resch-Genger, *Anal. Chem.* **2012**, *84*, 1345 – 1352.
[72] C. T. Xu, P. Svenmarker, H. C. Liu, X. Wu, M. E. Messing, L. R. Wallenberg, S. Andersson-Engels, *ACS Nano* **2012**, *6*, 4788 – 4795.
[73] J. C. Boyer, F. C. J. M. van Veggel, *Nanoscale* **2010**, *2*, 1417 – 1419.
[74] Q. Liu, T. S. Yang, W. Feng, F. Y. Li, *J. Am. Chem. Soc.* **2012**, *134*, 5390 – 5397.
[75] S. W. Wu, G. Han, D. J. Milliron, S. Aloni, V. Altoe, D. V. Talapin, B. E. Cohen, P. J. Schuck, *Proc. Natl. Acad. Sci. USA* **2009**, *106*, 10917 – 10921.
[76] D. E. Achatz, Dissertation, Universität Regensburg, **2012**.
[77] F. Wang, X. G. Liu, *J. Am. Chem. Soc.* **2008**, *130*, 5642 – 5643.
[78] F. Wang, R. Deng, J. Wang, Q. Wang, Y. Han, H. Zhu, X. Chen, X. Liu, *Nat. Mater.* **2011**, *10*, 968 – 973.
[79] O. Ehlert, R. Thomann, M. Darbandi, T. Nann, *ACS Nano* **2008**, *2*, 120 – 124.
[80] W. B. Niu, S. L. Wu, S. F. Zhang, J. Li, L. A. Li, *Dalton Trans.* **2011**, *40*, 3305 – 3314.
[81] W. B. Niu, S. L. Wu, S. F. Zhang, L. Li, *Chem. Commun.* **2010**, *46*, 3908 – 3910.
[82] W. B. Niu, S. L. Wu, S. F. Zhang, *J. Mater. Chem.* **2010**, *20*, 9113 – 9117.
[83] G. Y. Chen, H. C. Liu, G. Somesfalean, H. J. Liang, Z. G. Zhang, *Nanotechnology* **2009**, *20*, 385704.
[84] V. Mahalingam, R. Naccache, F. Vetrone, J. A. Capobianco, *Chem. Commun.* **2011**, *47*, 3481 – 3483.
[85] Q. Q. Dou, Y. Zhang, *Langmuir* **2011**, *27*, 13236 – 13241.
[86] J. Wang, F. Wang, C. Wang, Z. Liu, X. Liu, *Angew Chem.* **2011**, *123*, 10553 – 10556; *Angew Chem. Int. Ed.* **2011**, *50*, 10369 – 10372.
[87] F. Zhang, Q. H. Shi, Y. C. Zhang, Y. F. Shi, K. L. Ding, D. Y. Zhao, G. D. Stucky, *Adv. Mater.* **2011**, *23*, 3775 – 3779.
[88] F. Zhang, R. C. Haushalter, R. W. Haushalter, Y. Shi, Y. Zhang, K. Ding, D. Zhao, G. D. Stucky, *Small* **2011**, *7*, 1972 – 1976.
[89] R. E. Gerver, R. Gomez-Sjoberg, B. C. Baxter, K. S. Thorn, P. M. Fordyce, C. A. Diaz-Botia, B. A. Helms, J. L. DeRisi, *Lab Chip* **2012**, *12*, 4716 – 4723.
[90] H. H. Gorris, R. Ali, S. M. Saleh, O. S. Wolfbeis, *Adv. Mater.* **2011**, *23*, 1652 – 1655.
[91] Z. Q. Li, L. M. Wang, Z. Y. Wang, X. H. Liu, Y. J. Xiong, *J. Phys. Chem. C* **2011**, *115*, 3291 – 3296.
[92] Z. Q. Li, Y. Zhang, S. Jiang, *Adv. Mater.* **2008**, *20*, 4765 – 4769.
[93] L. A. Cheng, K. Yang, M. W. Shao, S. T. Lee, Z. A. Liu, *J. Phys. Chem. C* **2011**, *115*, 2686 – 2692.
[94] W. Q. Zou, C. Visser, J. A. Maduro, M. S. Pshenichnikov, J. C. Hummelen, *Nat. Photonics* **2012**, *6*, 560 – 564.
[95] F. Martínez Ferreras, O. S. Wolfbeis, H. H. Gorris, *Anal. Chim. Acta* **2012**, *729*, 62 – 66.
[96] S. Schietinger, T. Aichele, H. Q. Wang, T. Nann, O. Benson, *Nano Lett.* **2010**, *10*, 134 – 138.
[97] D. T. Tu, L. Q. Liu, Q. Ju, Y. S. Liu, H. M. Zhu, R. F. Li, X. Y. Chen, *Angew. Chem.* **2011**, *123*, 6430 – 6434; *Angew. Chem. Int. Ed.* **2011**, *50*, 6306 – 6310.
[98] Q. Ju, D. T. Tu, Y. S. Liu, R. F. Li, H. M. Zhu, J. C. Chen, Z. Chen, M. D. Huang, X. Y. Chen, *J. Am. Chem. Soc.* **2012**, *134*, 1323 – 1330.
[99] G. Z. Ren, S. J. Zeng, J. H. Hao, *J. Phys. Chem. C* **2011**, *115*, 20141 – 20147.
[100] Y. I. Park, J. H. Kim, K. T. Lee, K. S. Jeon, H. Bin Na, J. H. Yu, H. M. Kim, N. Lee, S. H. Choi, S. I. Baik, H. Kim, S. P. Park, B. J. Park, Y. W. Kim, S. H. Lee, S. Y. Yoon, I. C. Song, W. K. Moon, Y. D. Suh, T. Hyeon, *Adv. Mater.* **2009**, *21*, 4467 – 4471.
[101] H. C. Lu, G. S. Yi, S. Y. Zhao, D. P. Chen, L. H. Guo, J. Cheng, *J. Mater. Chem.* **2004**, *14*, 1336 – 1341.
[102] Z. Y. Liu, G. S. Yi, H. T. Zhang, J. Ding, Y. W. Zhang, J. M. Xue, *Chem. Commun.* **2008**, 694 – 696.
[103] C. C. Mi, J. P. Zhang, H. Y. Gao, X. L. Wu, M. Wang, Y. F. Wu, Y. Q. Di, Z. R. Xu, C. B. Mao, S. K. Xu, *Nanoscale* **2010**, *2*, 1141 – 1148.
[104] J. Shen, L. D. Sun, Y. W. Zhang, C. H. Yan, *Chem. Commun.* **2010**, *46*, 5731 – 5733.
[105] D. Jańczewski, Y. Zhang, G. K. Das, D. K. Yi, P. Padmanabhan, K. K. Bhakoo, T. T. Y. Tan, S. T. Selvan, *Microsc. Res. Tech.* **2011**, *74*, 563 – 576.
[106] E. Tóth, L. Helm, A. E. Merbach, *Top. Curr. Chem.* **2002**, *221*, 61 – 101.
[107] Z. Q. Li, Y. Zhang, B. Shuter, N. M. Idris, *Langmuir* **2009**, *25*, 12015 – 12018.
[108] F. Wang, Y. Han, C. S. Lim, Y. H. Lu, J. Wang, J. Xu, H. Y. Chen, C. Zhang, M. H. Hong, X. G. Liu, *Nature* **2010**, *463*, 1061 – 1065.
[109] Q. Liu, Y. Sun, T. S. Yang, W. Feng, C. G. Li, F. Y. Li, *J. Am. Chem. Soc.* **2011**, *133*, 17122 – 17125.
[110] P. A. Tanner, J. W. Wang, *Chem. Phys. Lett.* **2008**, *455*, 335 – 338.
[111] R. Komban, J. P. Klare, B. Voss, J. Nordmann, H. J. Steinhoff, M. Haase, *Angew. Chem.* **2012**, *124*, 6612 – 6616; *Angew. Chem. Int. Ed.* **2012**, *51*, 6506 – 6510.
[112] D. Q. Chen, Y. L. Yu, F. Huang, A. P. Yang, Y. S. Wang, *J. Mater. Chem.* **2011**, *21*, 6186 – 6192.
[113] R. Kumar, M. Nyk, T. Y. Ohulchanskyy, C. A. Flask, P. N. Prasad, *Adv. Funct. Mater.* **2009**, *19*, 853 – 859.
[114] Y. L. Liu, K. L. Ai, J. H. Liu, Q. H. Yuan, Y. Y. He, L. H. Lu, *Angew. Chem.* **2012**, *124*, 1466 – 1471; *Angew. Chem. Int. Ed.* **2012**, *51*, 1437 – 1442.
[115] G. Zhang, Y. L. Liu, Q. H. Yuan, C. H. Zong, J. H. Liu, L. H. Lu, *Nanoscale* **2011**, *3*, 4365 – 4371.
[116] Q. Liu, Y. Sun, C. G. Li, J. Zhou, C. Y. Li, T. S. Yang, X. Z. Zhang, T. Yi, D. M. Wu, F. Y. Li, *ACS Nano* **2011**, *5*, 3146 – 3157.
[117] C. X. Li, J. Lin, *J. Mater. Chem.* **2010**, *20*, 6831 – 6847.
[118] G. S. Yi, H. C. Lu, S. Y. Zhao, G. Yue, W. J. Yang, D. P. Chen, L. H. Guo, *Nano Lett.* **2004**, *4*, 2191 – 2196.
[119] H. X. Mai, Y. W. Zhang, R. Si, Z. G. Yan, L. D. Sun, L. P. You, C. H. Yan, *J. Am. Chem. Soc.* **2006**, *128*, 6426 – 6436.
[120] J. N. Shan, Y. G. Ju, *Nanotechnology* **2009**, *20*, 275603.
[121] J. H. Zeng, J. Su, Z. H. Li, R. X. Yan, Y. D. Li, *Adv. Mater.* **2005**, *17*, 2119 – 2123.
[122] C. Liu, H. Wang, X. Li, D. Chen, *J. Mater. Chem.* **2009**, *19*, 3546 – 3553.
[123] L. Y. Wang, Y. D. Li, *Chem. Mater.* **2007**, *19*, 727 – 734.
[124] X. M. Liu, J. W. Zhao, Y. J. Sun, K. Song, Y. Yu, C. A. Du, X. G. Kong, H. Zhang, *Chem. Commun.* **2009**, 6628 – 6630.
[125] M. Longmire, P. L. Choyke, H. Kobayashi, *Nanomedicine* **2008**, *3*, 703 – 717.
[126] G. Y. Chen, T. Y. Ohulchanskyy, R. Kumar, H. Agren, P. N. Prasad, *ACS Nano* **2010**, *4*, 3163 – 3168.
[127] H. T. Wong, F. Vetrone, R. Naccache, H. L. W. Chan, J. H. Hao, J. A. Capobianco, *J. Mater. Chem.* **2011**, *21*, 16589 – 16596.

[128] A. D. Ostrowski, E. M. Chan, D. J. Gargas, E. M. Katz, G. Han, P. J. Schuck, D. J. Milliron, B. E. Cohen, *ACS Nano* **2012**, *6*, 2686 – 2692.
[129] W. R. Algar, D. E. Prasuhn, M. H. Stewart, T. L. Jennings, J. B. Blanco-Canosa, P. E. Dawson, I. L. Medintz, *Bioconjugate Chem.* **2011**, *22*, 825 – 858.
[130] H. Schäfer, P. Ptacek, K. Kömpe, M. Haase, *Chem. Mater.* **2007**, *19*, 1396 – 1400.
[131] Q. B. Zhang, K. Song, J. W. Zhao, X. G. Kong, Y. J. Sun, X. M. Liu, Y. L. Zhang, Q. H. Zeng, H. Zhang, *J. Colloid Interface Sci.* **2009**, *336*, 171 – 175.
[132] G. S. Yi, G. M. Chow, *Adv. Funct. Mater.* **2006**, *16*, 2324 – 2329.
[133] L. Q. Xiong, T. S. Yang, Y. Yang, C. J. Xu, F. Y. Li, *Biomaterials* **2010**, *31*, 7078 – 7085.
[134] N. J. J. Johnson, N. M. Sangeetha, J. C. Boyer, F. C. J. M. van Veggel, *Nanoscale* **2010**, *2*, 771 – 777.
[135] Z. Q. Li, Y. Zhang, *Angew. Chem.* **2006**, *118*, 7896 – 7899; *Angew. Chem. Int. Ed.* **2006**, *45*, 7732 – 7735.
[136] S. J. Budijono, J. N. Shan, N. Yao, Y. Miura, T. Hoye, R. H. Austin, Y. G. Ju, R. K. Prud'homme, *Chem. Mater.* **2010**, *22*, 311 – 318.
[137] L. L. Li, R. B. Zhang, L. L. Yin, K. Z. Zheng, W. P. Qin, P. R. Selvin, Y. Lu, *Angew. Chem.* **2012**, *124*, 6225 – 6229; *Angew. Chem. Int. Ed.* **2012**, *51*, 6121 – 6125.
[138] Z. G. Chen, H. L. Chen, H. Hu, M. X. Yu, F. Y. Li, Q. Zhang, Z. G. Zhou, T. Yi, C. H. Huang, *J. Am. Chem. Soc.* **2008**, *130*, 3023 – 3029.
[139] N. Bogdan, F. Vetrone, G. A. Ozin, J. A. Capobianco, *Nano Lett.* **2011**, *11*, 835 – 840.
[140] R. A. Jalil, Y. Zhang, *Biomaterials* **2008**, *29*, 4122 – 4128.
[141] J. N. Shan, Y. G. Ju, *Appl. Phys. Lett.* **2007**, *91*, 123103.
[142] C. Louis, R. Bazzi, C. A. Marquette, J. L. Bridot, S. Roux, G. Ledoux, B. Mercier, L. Blum, P. Perriat, O. Tillement, *Chem. Mater.* **2005**, *17*, 1673 – 1682.
[143] S. Sivakumar, P. R. Diamente, F. C. van Veggel, *Chem. Eur. J.* **2006**, *12*, 5878 – 5884.
[144] H. Hu, L. Q. Xiong, J. Zhou, F. Y. Li, T. Y. Cao, C. H. Huang, *Chem. Eur. J.* **2009**, *15*, 3577 – 3584.
[145] L. Cheng, K. Yang, Y. G. Li, J. H. Chen, C. Wang, M. W. Shao, S. T. Lee, Z. Liu, *Angew. Chem.* **2011**, *123*, 7523 – 7528; *Angew. Chem. Int. Ed.* **2011**, *50*, 7385 – 7390.
[146] T. Zako, H. Nagata, N. Terada, A. Utsumi, M. Sakono, M. Yohda, H. Ueda, K. Soga, M. Maeda, *Biochem. Biophys. Res. Commun.* **2009**, *381*, 54 – 58.
[147] D. Y. Kong, Z. W. Quan, J. Yang, P. P. Yang, C. X. Li, J. Lin, *J. Nanopart. Res.* **2009**, *11*, 821 – 829.
[148] S. M. Saleh, R. Ali, T. Hirsch, O. S. Wolfbeis, *J. Nanopart. Res.* **2011**, *13*, 4603 – 4611.
[149] M. Wang, W. Hou, C. C. Mi, W. X. Wang, Z. R. Xu, H. H. Teng, C. B. Mao, S. K. Xu, *Anal. Chem.* **2009**, *81*, 8783 – 8789.
[150] M. Wang, C. C. Mi, W. X. Wang, C. H. Liu, Y. F. Wu, Z. R. Xu, C. B. Mao, S. K. Xu, *ACS Nano* **2009**, *3*, 1580 – 1586.
[151] S. Jiang, Y. Zhang, *Langmuir* **2010**, *26*, 6689 – 6694.
[152] L. Y. Wang, Y. D. Li, *Chem. Commun.* **2006**, 2557 – 2559.
[153] H. S. Mader, M. Link, D. E. Achatz, K. Uhlmann, X. H. Li, O. S. Wolfbeis, *Chem. Eur. J.* **2010**, *16*, 5416 – 5424.
[154] M. M. Rubner, D. E. Achatz, H. S. Mader, J. A. Stolwijk, J. Wegener, G. S. Harms, O. S. Wolfbeis, H. A. Wagenknecht, *ChemPlusChem* **2012**, *77*, 129 – 134.
[155] F. Wang, D. Banerjee, Y. S. Liu, X. Y. Chen, X. G. Liu, *Analyst* **2010**, *135*, 1839 – 1854.
[156] D. K. Chatterjee, A. J. Rufalhah, Y. Zhang, *Biomaterials* **2008**, *29*, 937 – 943.
[157] M. Nyk, R. Kumar, T. Y. Ohulchanskyy, E. J. Bergey, P. N. Prasad, *Nano Lett.* **2008**, *8*, 3834 – 3838.
[158] J. Pichaandi, J. C. Boyer, K. R. Delaney, F. C. J. M. van Veggel, *J. Phys. Chem. C* **2011**, *115*, 19054 – 19064.
[159] C. J. Carling, J. C. Boyer, N. R. Branda, *J. Am. Chem. Soc.* **2009**, *131*, 10838 – 10839.
[160] C. J. Carling, F. Nourmohammadian, J. C. Boyer, N. R. Branda, *Angew. Chem.* **2010**, *122*, 3870 – 3873; *Angew. Chem. Int. Ed.* **2010**, *49*, 3782 – 3785.
[161] Y. M. Yang, Q. Shao, R. R. Deng, C. Wang, X. Teng, K. Cheng, Z. Cheng, L. Huang, Z. Liu, X. G. Liu, B. G. Xing, *Angew. Chem.* **2012**, *124*, 3179 – 3183; *Angew. Chem. Int. Ed.* **2012**, *51*, 3125 – 3129.
[162] M. K. G. Jayakumar, N. M. Idris, Y. Zhang, *Proc. Natl. Acad. Sci. USA* **2012**, *109*, 8483 – 8488.
[163] J. V. Garcia, J. Yang, D. Shen, C. Yao, X. Li, R. Wang, G. D. Stucky, D. Zhao, P. C. Ford, F. Zhang, *Small* **2012**, *8*, 3800 – 3805.
[164] P. Zhang, W. Steelant, M. Kumar, M. Scholfield, *J. Am. Chem. Soc.* **2007**, *129*, 4526
[165] C. Wang, H. Q. Tao, L. Cheng, Z. Liu, *Biomaterials* **2011**, *32*, 6145 – 6154.
[166] K. Liu, X. M. Liu, Q. H. Zeng, Y. L. Zhang, L. P. Tu, T. Liu, X. G. Kong, Y. H. Wang, F. Cao, S. A. G. Lambrechts, M. C. G. Aalders, H. Zhang, *ACS Nano* **2012**, *6*, 4054 – 4062.
[167] S. F. Lim, R. Riehn, W. S. Ryu, N. Khanarian, C. K. Tung, D. Tank, R. H. Austin, *Nano Lett.* **2006**, *6*, 169 – 174.
[168] S. F. Lim, R. Riehn, C. K. Tung, W. S. Ryu, R. Zhuo, J. Dalland, R. H. Austin, *Nanotechnology* **2009**, *20*, 405701.
[169] J. Chen, C. R. Guo, M. Wang, L. Huang, L. P. Wang, C. C. Mi, J. Li, X. X. Fang, C. B. Mao, S. K. Xu, *J. Mater. Chem.* **2011**, *21*, 2632 – 2638.
[170] Z. L. Wang, J. H. Hao, H. L. W. Chan, G. L. Law, W. T. Wong, K. L. Wong, M. B. Murphy, T. Su, Z. H. Zhang, S. Q. Zeng, *Nanoscale* **2011**, *3*, 2175 – 2181.
[171] A. Hischemöller, J. Nordmann, P. Ptacek, K. Mummenhoff, M. Haase, *J. Biomed. Nanotechnol.* **2009**, *5*, 278 – 284.
[172] J. Zhou, Z. Liu, F. Y. Li, *Chem. Soc. Rev.* **2012**, *41*, 1323 – 1349.
[173] S. A. Hilderbrand, F. W. Shao, C. Salthouse, U. Mahmood, R. Weissleder, *Chem. Commun.* **2009**, 4188 – 4190.
[174] H. Kobayashi, N. Kosaka, M. Ogawa, N. Y. Morgan, P. D. Smith, C. B. Murray, X. C. Ye, J. Collins, G. A. Kumar, H. Bell, P. L. Choyke, *J. Mater. Chem.* **2009**, *19*, 6481 – 6484.
[175] L. A. Cheng, K. Yang, S. A. Zhang, M. W. Shao, S. T. Lee, Z. A. Liu, *Nano Res.* **2010**, *3*, 722 – 732.
[176] J. F. Jin, Y. J. Gu, C. W. Y. Man, J. P. Cheng, Z. H. Xu, Y. Zhang, H. S. Wang, V. H. Y. Lee, S. H. Cheng, W. T. Wong, *ACS Nano* **2011**, *5*, 7838 – 7847.
[177] X. F. Yu, M. Li, M. Y. Xie, L. D. Chen, Y. Li, Q. Q. Wang, *Nano Res.* **2010**, *3*, 51 – 60.
[178] S. Jeong, N. Won, J. Lee, J. Bang, J. Yoo, S. G. Kim, J. A. Chang, J. Kim, S. Kim, *Chem. Commun.* **2011**, *47*, 8022 – 8024.
[179] J. N. Shan, J. B. Chen, J. Meng, J. Collins, W. Soboyejo, J. S. Friedberg, Y. G. Ju, *J. Appl. Phys.* **2008**, *104*, 094308.
[180] M. X. Yu, F. Y. Li, Z. G. Chen, H. Hu, C. Zhan, H. Yang, C. H. Huang, *Anal. Chem.* **2009**, *81*, 930 – 935.
[181] F. Vetrone, R. Naccache, A. J. de La Fuente, F. Sanz-Rodriguez, A. Blazquez-Castro, E. M. Rodriguez, D. Jaque, J. G. Sole, J. A. Capobianco, *Nanoscale* **2010**, *2*, 495 – 498.
[182] S. H. Nam, Y. M. Bae, Y. I. Park, J. H. Kim, H. M. Kim, J. S. Choi, K. T. Lee, T. Hyeon, Y. D. Suh, *Angew. Chem.* **2011**, *123*, 6217 – 6221; *Angew. Chem. Int. Ed.* **2011**, *50*, 6093 – 6097.
[183] L. Q. Xiong, Z. G. Chen, M. X. Yu, F. Y. Li, C. Liu, C. H. Huang, *Biomaterials* **2009**, *30*, 5592 – 5600.
[184] P. S. Low, W. A. Henne, D. D. Doorneweerd, *Acc. Chem. Res.* **2008**, *41*, 120 – 129.
[185] X. F. Yu, Z. B. Sun, M. Li, Y. Xiang, Q. Q. Wang, F. F. Tang, Y. L. Wu, Z. J. Cao, W. X. Li, *Biomaterials* **2010**, *31*, 8724 – 8731.
[186] L. Q. Xiong, Z. G. Chen, Q. W. Tian, T. Y. Cao, C. J. Xu, F. Y. Li, *Anal. Chem.* **2009**, *81*, 8687 – 8694.

[187] Q. Q. Zhan, J. Qian, H. J. Liang, G. Somesfalean, D. Wang, S. L. He, Z. G. Zhang, S. Andersson-Engels, *ACS Nano* **2011**, *5*, 3744 – 3757.
[188] G. S. Yi, Y. F. Peng, Z. Q. Gao, *Chem. Mater.* **2011**, *23*, 2729 – 2734.
[189] S. Jiang, Y. Zhang, K. M. Lim, E. K. W. Sim, L. Ye, *Nanotechnology* **2009**, *20*, 155101.
[190] M. Wang, C. C. Mi, Y. X. Zhang, J. L. Liu, F. Li, C. B. Mao, S. K. Xu, *J. Phys. Chem. C* **2009**, *113*, 19021 – 19027.
[191] X. D. Wang, H. H. Gorris, J. A. Stolwijk, R. J. Meier, D. B. M. Groegel, J. Wegener, O. S. Wolfbeis, *Chem. Sci.* **2011**, *2*, 901 – 906.
[192] M. Schäferling, *Angew. Chem.* **2012**, *124*, 3590 – 3614; *Angew. Chem. Int. Ed.* **2012**, *51*, 3532 – 3554.
[193] F. Vetrone, R. Naccache, A. Zamarron, A. J. de La Fuente, F. Sanz-Rodriguez, L. M. Maestro, E. M. Rodriguez, D. Jaque, J. G. Sole, J. A. Capobianco, *ACS Nano* **2010**, *4*, 3254 – 3258.
[194] B. Dong, B. S. Cao, Y. Y. He, Z. Liu, Z. P. Li, Z. Q. Feng, *Adv. Mater.* **2012**, *24*, 1987 – 1993.
[195] D. E. Achatz, R. Ali, O. S. Wolfbeis, *Topics Curr. Chem.* **2010**, *300*, 29 – 50.
[196] H. J. M. A. A. Zijlmans, J. Bonnet, J. Burton, K. Kardos, T. Vail, R. S. Niedbala, H. J. Tanke, *Anal. Biochem.* **1999**, *267*, 30 – 36.
[197] F. van de Rijke, H. Zijlmans, S. Li, T. Vail, A. K. Raap, R. S. Niedbala, H. J. Tanke, *Nat. Biotechnol.* **2001**, *19*, 273 – 276.
[198] P. L. A. M. Corstjens, M. Zuiderwijk, M. Nilsson, H. Feindt, R. S. Niedbala, H. J. Tanke, *Anal. Biochem.* **2003**, *312*, 191 – 200.
[199] P. Corstjens, M. Zuiderwijk, A. Brink, S. Li, H. Feindt, R. S. Neidbala, H. Tanke, *Clin. Chem.* **2001**, *47*, 1885 – 1893.
[200] P. L. A. M. Corstjens, L. van Lieshout, M. Zuiderwijk, D. Kornelis, H. J. Tanke, A. M. Deelder, G. J. van Dam, *J. Clin. Microbiol.* **2008**, *46*, 171 – 176.
[201] C. C. Liu, X. B. Qiu, S. Ongagna, D. F. Chen, Z. Y. Chen, W. R. Abrams, D. Malamud, P. L. A. M. Corstjens, H. H. Bau, *Lab Chip* **2009**, *9*, 768 – 776.
[202] P. L. A. M. Corstjens, M. Zuiderwijk, H. J. Tanke, J. J. V. V. Schip, T. H. M. Ottenhoff, A. Geluk, *Clin. Biochem.* **2008**, *41*, 440 – 444.
[203] J. Hampl, M. Hall, N. A. Mufti, Y. M. M. Yao, D. B. MacQueen, W. H. Wright, D. E. Cooper, *Anal. Biochem.* **2001**, *288*, 176 – 187.
[204] R. S. Niedbala, H. Feindt, K. Kardos, T. Vail, J. Burton, B. Bielska, S. Li, D. Milunic, P. Bourdelle, R. Vallejo, *Anal. Biochem.* **2001**, *293*, 22 – 30.
[205] P. L. A. M. Corstjens, Z. Y. Chen, M. Zuiderwijk, H. H. Bau, W. R. Abrams, D. Malamud, R. S. Niedbala, H. J. Tanke, *Ann. N. Y. Acad. Sci.* **2007**, *1098*, 437 – 445.
[206] K. Kuningas, T. Rantanen, U. Karhunen, T. Lövgren, T. Soukka, *Anal. Chem.* **2005**, *77*, 2826 – 2834.
[207] K. Kuningas, T. Rantanen, T. Lövgren, T. Soukka, *Anal. Chim. Acta* **2005**, *543*, 130 – 136.
[208] T. Ukonaho, T. Rantanen, L. Jämsen, K. Kuningas, H. Päkkilä, T. Lövgren, T. Soukka, *Anal. Chim. Acta* **2007**, *596*, 106 – 115.
[209] M. Ylihärsilä, T. Valta, M. Karp, L. Hattara, E. Harju, J. Hölsä, P. Saviranta, M. Waris, T. Soukka, *Anal. Chem.* **2011**, *83*, 1456 – 1461.
[210] D. E. Cooper, A. D'Andrea, G. W. Faris, D. B. MacQueen, W. H. Wright, *Immunoassays and other bioanalytical techniques* (Ed.: J. M. Van Emon), CRC, Boca Raton, **2007**.
[211] K. Kuningas, T. Rantanen, T. Ukonaho, T. Lövgren, T. Soukka, *Anal. Chem.* **2005**, *77*, 7348 – 7355.
[212] T. Rantanen, H. Päkkilä, L. Jämsen, K. Kuningas, T. Ukonaho, T. Lövgren, T. Soukka, *Anal. Chem.* **2007**, *79*, 6312 – 6318.
[213] K. Kuningas, T. Ukonaho, H. Päkkilä, T. Rantanen, J. Rosenberg, T. Lövgren, T. Soukka, *Anal. Chem.* **2006**, *78*, 4690 – 4696.
[214] T. Soukka, T. Rantanen, K. Kuningas, *Ann. N. Y. Acad. Sci.* **2008**, *1130*, 188 – 200.
[215] L. Y. Wang, R. X. Yan, Z. Y. Hao, L. Wang, J. H. Zeng, H. Bao, X. Wang, Q. Peng, Y. D. Li, *Angew. Chem.* **2005**, *117*, 6208 – 6211; *Angew. Chem. Int. Ed.* **2005**, *44*, 6054 – 6057.
[216] J. H. Peng, Y. H. Wang, J. L. Wang, X. Zhou, Z. H. Liu, *Biosens. Bioelectron.* **2011**, *28*, 414 – 420.
[217] A. Bednarkiewicz, M. Nyk, M. Samoc, W. Strek, *J. Phys. Chem. C* **2010**, *114*, 17535 – 17541.
[218] Y. H. Wang, L. Bao, Z. H. Liu, D. W. Pang, *Anal. Chem.* **2011**, *83*, 8130 – 8137.
[219] Y. H. Wang, P. Shen, C. Y. Li, Y. Y. Wang, Z. H. Liu, *Anal. Chem.* **2012**, *84*, 1466 – 1473.
[220] C. L. Zhang, Y. X. Yuan, S. M. Zhang, Y. H. Wang, Z. H. Liu, *Angew. Chem.* **2011**, *123*, 6983 – 6986; *Angew. Chem. Int. Ed.* **2011**, *50*, 6851 – 6854.
[221] R. R. Deng, X. J. Xie, M. Vendrell, Y. T. Chang, X. G. Liu, *J. Am. Chem. Soc.* **2011**, *133*, 20168 – 20171.
[222] F. Vetrone, R. Naccache, C. G. Morgan, J. A. Capobianco, *Nanoscale* **2010**, *2*, 1185 – 1189.
[223] P. R. Selvin, T. M. Rana, J. E. Hearst, *J. Am. Chem. Soc.* **1994**, *116*, 6029 – 6030.
[224] T. Rantanen, M. L. Jarvenpaa, J. Vuojola, K. Kuningas, T. Soukka, *Angew. Chem.* **2008**, *120*, 3871 – 3873; *Angew. Chem. Int. Ed.* **2008**, *47*, 3811 – 3813.
[225] Y. X. Yuan, Z. H. Liu, *Chem. Commun.* **2012**, *48*, 7510 – 7512.
[226] P. Zhang, S. Rogelj, K. Nguyen, D. Wheeler, *J. Am. Chem. Soc.* **2006**, *128*, 12410 – 12411.
[227] M. Kumar, Y. Guo, P. Zhang, *Biosens. Bioelectron.* **2009**, *24*, 1522 – 1526.
[228] M. Kumar, P. Zhang, *Langmuir* **2009**, *25*, 6024 – 6027.
[229] T. Rantanen, M. L. Järvenpää, J. Vuojola, R. Arppe, K. Kuningas, T. Soukka, *Analyst* **2009**, *134*, 1713 – 1716.
[230] K. Kuningas, H. Päkkilä, T. Ukonaho, T. Rantanen, T. Lövgren, T. Soukka, *Clin. Chem.* **2007**, *53*, 145 – 146.
[231] N. Bogdan, F. Vetrone, R. Roy, J. A. Capobianco, *J. Mater. Chem.* **2010**, *20*, 7543 – 7550.
[232] K. Song, X. G. Kong, X. M. Liu, Y. L. Zhang, Q. H. Zeng, L. P. Tu, Z. Shi, H. Zhang, *Chem. Commun.* **2012**, *48*, 1156 – 1158.
[233] H. H. Gorris, S. Bade, N. Röckendorf, E. Albers, M. A. Schmidt, M. Franek, A. Frey, *Anal. Chem.* **2009**, *81*, 1580 – 1586.
[234] J. Vuojola, T. Riuttamaki, E. Kulta, R. Arppe, T. Soukka, *Anal. Chim. Acta* **2012**, *725*, 67 – 73.
[235] H. S. Mader, O. S. Wolfbeis, *Anal. Chem.* **2010**, *82*, 5002 – 5004.
[236] R. Ali, S. M. Saleh, R. J. Meier, H. A. Azab, I. I. Abdelgawad, O. S. Wolfbeis, *Sens. Actuators B* **2010**, *150*, 126 – 131.
[237] D. E. Achatz, R. J. Meier, L. H. Fischer, O. S. Wolfbeis, *Angew. Chem.* **2011**, *123*, 274 – 277; *Angew. Chem. Int. Ed.* **2011**, *50*, 260 – 263.
[238] L. N. Sun, H. S. Peng, M. I. J. Stich, D. Achatz, O. S. Wolfbeis, *Chem. Commun.* **2009**, 5000 – 5002.
[239] M. Kumar, P. Zhang, *Biosens. Bioelectron.* **2010**, *25*, 2431 – 2435.
[240] W. J. Kim, M. Nyk, P. N. Prasad, *Nanotechnology* **2009**, *20*, 185301.
[241] Y. L. Liu, K. L. Ai, L. H. Lu, *Nanoscale* **2011**, *3*, 4804 – 4810.
[242] J. M. Meruga, W. M. Cross, P. S. May, Q. Luu, G. A. Crawford, J. J. Kellar, *Nanotechnology* **2012**, *23*, 395201.
[243] A. L. Ouellette, J. J. Li, D. E. Cooper, A. J. Ricco, G. T. A. Kovacs, *Anal. Chem.* **2009**, *81*, 3216 – 3221.